Integrated Pest Management: Advancement, Adoption and Ecological Challenges
DOI: https://doi.org/10.54083/978-81-986377-3-4_03

Chapter_3

Latest Improvements in Insect Pheromonal Research, Method and Protocols

Gogoi, J.[1*], Ningthoujam, K.[1], Pathak, M.[1], Ng. Tombisana Meetei[2] and Sorokhaibam, M.[1]

[1]Dept. of Entomology, [2]Dept. of Plant Molecular Biology and Biotechnology, School of Crop Protection, College of Post Graduate Studies in Agricultural Sciences, Central Agricultural University (Imphal), Umiam, Meghalaya (793 103), India

Abstract

A pheromone is a chemical or a mixture of chemicals emitted by an organism that triggers specific reactions in another individual of the same species (Shorey, 1977). Semiochemicals, which include pheromones and allelochemicals, serve as markers or signals to convey information between individuals of the same species or different species. Allelochemicals can be classified based on their effects: kairomones (beneficial to the receiver), synomones (beneficial to both the emitter and the receiver), allomones (beneficial to the emitter) and apneumones (of nonbiological origin). Recent advancements in pheromone technology include eco-friendly delivery systems, electrochemical detection and innovative applications. For example, Chen *et al.* (2018) developed a controlled-release system using sex pheromone-loaded MPEG-PCL diblock copolymer micelles for Spodoptera litura. Researchers are also exploring nanocomposites and polymers to prolong the release of volatile organic compounds for pest and disease control. Stipanovic *et al.* (2004) studied micrometer-sized particles for controlled release of insect pheromones, using codlemone/1-dodecanol and disparlure/1,2-epoxyoctadecane as model compounds. Molecular gels are being investigated for their potential in creating efficient controlled-release devices for pheromones, offering high loading capacity and sustained release (Jadhav *et al.*, 2010). Additionally, Hellmann *et al.* (2009) developed pheromone-releasing nanofibers for plant protection using electrospinning of polyamide, which provide extended release over weeks or months. For detecting and characterizing insect pheromones, various novel methods are available, such as Gas Chromatography (GC), Direct Analysis in Real Time Mass Spectrometry (DART-MS), Matrix-Assisted Laser Desorption/Ionization Mass Spectrometry (MALDI), Electrospray Ionization Mass Spectrometry (ESI-MS) and Gas Chromatography coupled with Electroantennogram Detection (GC-EAD). Behavioral studies of insects can be conducted using wind tunnels and olfactometer bioassays to test essential oils against pests like *Helopeltis theivora*. This chapter will explore the detection and quantification of pheromones, along with modern equipment, biosensors and other recent developments in pheromone technology.

[*]***Corresponding author's e-mail***: jyotimgogoi@gmail.com

How to cite:
Gogoi, J., Ningthoujam, K., Pathak, M., Meetei, N.T., Sorokhaibam, M., 2025. Latest improvements in insect pheromonal research, method and protocols. In: *Integrated Pest Management: Advancement, Adoption and Ecological Challenges.* (Ed.) Sehgal, M. Biotica Publications, India. pp. 25-61. DOI: https://doi.org/10.54083/978-81-986377-3-4_03.

Keywords Cantilever, Gas sensor, VOCs, Electrochemical detection, Nanocomposite, Molecular gels, Controlled release, nanofibers, Microparticle dispensers

1. Introduction

The term "pheromone" is derived from the Greek words "phereum," meaning to carry and "horman," meaning to excite. Pheromones are chemicals secreted by specialized glands of one animal, which then influence another individual of the same species. These chemicals are typically active in very low concentrations and usually exist as a blend of compounds specific to each species. Pheromones can be categorized based on their mode of action. Releaser pheromones trigger an immediate and reversible behavioral response in the receiver, mediated by the nervous system shortly after detection. These pheromones influence various insect behaviors. In contrast, primer pheromones induce a more fundamental physiological change in the receiver, altering its response by acting directly on the nervous system or other physiological systems. Types of primer pheromones include sex pheromones, aggregation pheromones, alarm pheromones, trail pheromones and dispersal or spacing pheromones.

Insects' growth and development are regulated by several hormones secreted by the endocrine system's ductless glands. These hormones include Brain Hormone (BH) or Prothoracicotropic Hormone (PTTH), Moulting Hormones (MH), Juvenile Hormones (JH), Eclosion Hormone (EH) and Tanning Hormone (TH) (Pedigo, 2003). BH/PTTH is generated by neurosecretory cells in the brain and stimulates the prothoracic glands, which then produce ecdysone, a hormone essential for molting.

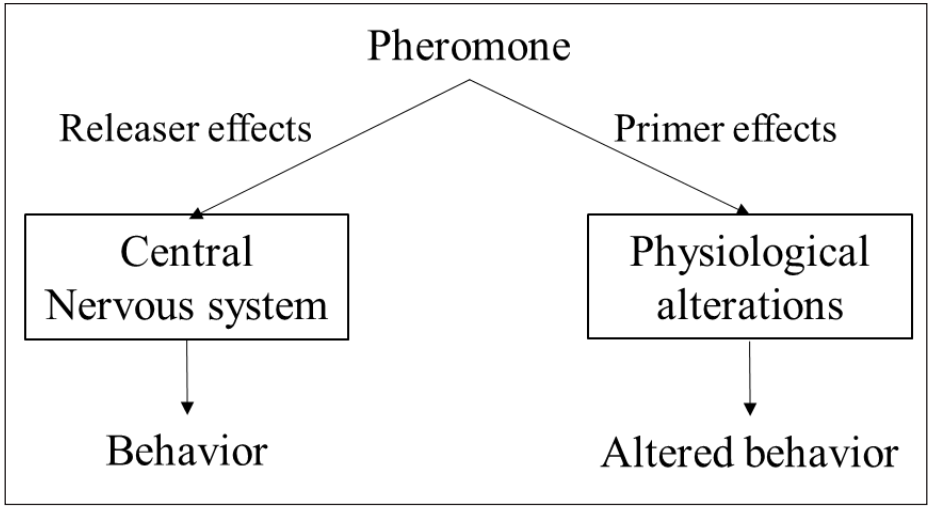

2. Chemical Structure

Lipid-based insect pheromones encompass a range of both volatile and non-volatile signals. Many of these pheromones originate from a single source, such as fatty acids or isoprenes, with slight modifications to the main structure. Common modifications include adding functional groups to create alcohols, aldehydes, acetates or epoxides/ketones, incorporating branched fatty acids or amino acids or altering stereochemistry. The position of double bonds in these molecules is crucial for signaling; the exact placement of double bonds can vary among closely related species and is often the key to a pheromone's species specificity and function. For instance, the green-headed leaf roller *Planotortrix excessana* produces (Z)-5- and (Z)-7-tetradecenyl acetate, while its close relative *P. octo* produces (Z)-8- and (Z)-10-tetradecenyl acetate. Similar examples of double bond regioisomerism are observed in other leaf roller species pairs. In other lepidopteran species, sex pheromones also achieve specificity through complex blends of polyenes with 2 to 4 unsaturation sites (Yew and Chung, 2015).

In moths, changes in the ratio of stereoisomers can contribute to the formation of new type of pheromone. For instance, regional variants of the European corn borer moth (*Ostrinia nubilalis*) are distinguished by different blends of the female sex pheromone, specifically (E)-11- and (Z)-11-tetradecenyl acetate. One variant has a 98:2 E/Z molar ratio, while another has a 3:97 E/Z molar ratio. Additionally, minor variations in pheromone length can influence the specificity of the resulting behavior. For example, in *Drosophila melanogaster*, the 23-carbon monoene (Z)-7-tricosene inhibits male-male courtship and is crucial for male-male aggression, whereas the slightly longer 25-carbon monoene (Z)-7-pentacosene does not have this effect (Yew and Chung 2015). To identify these chemical structures and their specific stereochemical properties, advanced techniques like solvent extraction and chromatography are used. Examples of these components include linear aliphatic and (hetero)cyclic compounds, as detailed in tables 1 and 2.

3. Analytical Methods for Detection and Characterization of Insect Pheromone

The method for extracting pheromones should be customized based on the morphological, biological and behavioral traits of the insects being studied, as well as the chemical nature of the released compounds (Anderson *et al.*, 2009). Common techniques for pheromone extraction include aeration (volatile collection) and solvent extraction (Millar and Haynes, 2000). In air-entrainment volatile collection, the volatiles emitted by the insects over a specified period are captured using a small amount (50-200 mg) of a polymeric adsorbent, such as activated carbon, Porapak Q, Tenax GR or Tenax TA. These volatiles are then adsorbed onto the polymers and later desorbed with organic solvents like ethyl ether, hexane and dichloromethane. This technique is beneficial because it allows for the extraction of pheromones from live insects over a controlled timeframe and is especially useful for

Table 1: Examples of insect pheromones and their function in social behaviors

Sl. No.	Function		Species	Structure
1	Attraction and mating	Aphrodisiac	Silkmoth (*Bombyx mori*)	Bombykol
			German cockroach (*Blattella germanica*)	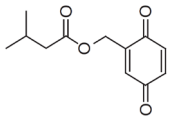
				Blattellaquinone
2		Species recognition	Vinegar flies (*Drosophila*)	
				(Z)-7-tricosene
3		Antiaphr-odisiac	*D. mojavensis* and *D. arizonae*	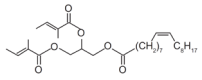
				1, 2-ditigloyl-3-oleoylglycerol
4	Aggregation		Ambrosia beetle (*Gnathotrichus sulcatus*)	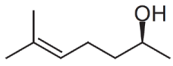
				(S)-sulcatol
				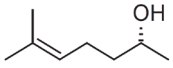
				(R)-sulcatol
5	Alarm		Aphids	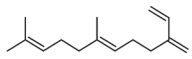
				(E)- -farnesene
			Honey bee	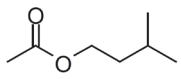
				Isopentyl acetate
6	Defense		Arctiidae moth (*Cosmosoma myrodora*)	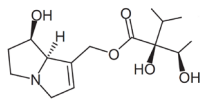
				Intermedine

Sl. No.	Function	Species	Structure
			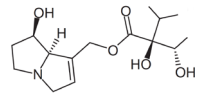 Lycopsamine
7	Social hierarchy	Honey bee (*Apis mellifera*)	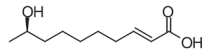 (R,E)-(-)-9-HDA
			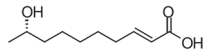 (S,E)-(+)-9-HAD (Hydroxyl-2-enoic acid)
			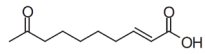 (E)-9-ODA (Oxodec-2-enoic acid)
			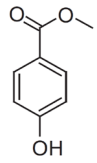 HOB (Methyl 4-hydroxybenzoate)
			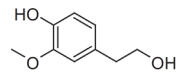 HVA (Homovanillyl alcohol)

pheromones not stored in specific glands or compartments. Additionally, Solid-Phase Microextraction (SPME) is another method used to extract semiochemicals from insects. SPME involves adsorbing the analyte onto a very thin (7-100 μm) polymeric film that coats a silica capillary fiber (Augusto and Valente, 2002).

The strategy for the study of volatile semiochemicals of insects is (McCafferyand Wilson 1990):

a) Obtain evidence for semiochemical production in laboratory or field behavioral bioassay experiments.

Table 2: A variety of female and male sex pheromones from lepidopteran species highlight the wide range and complexity of their chemical structures. These include: a) acetates, alcohols and aldehydes; b) esters, ketones and epoxides; c) hydrocarbons; d) terpenoids; and e) cyclic and heterocyclic compounds

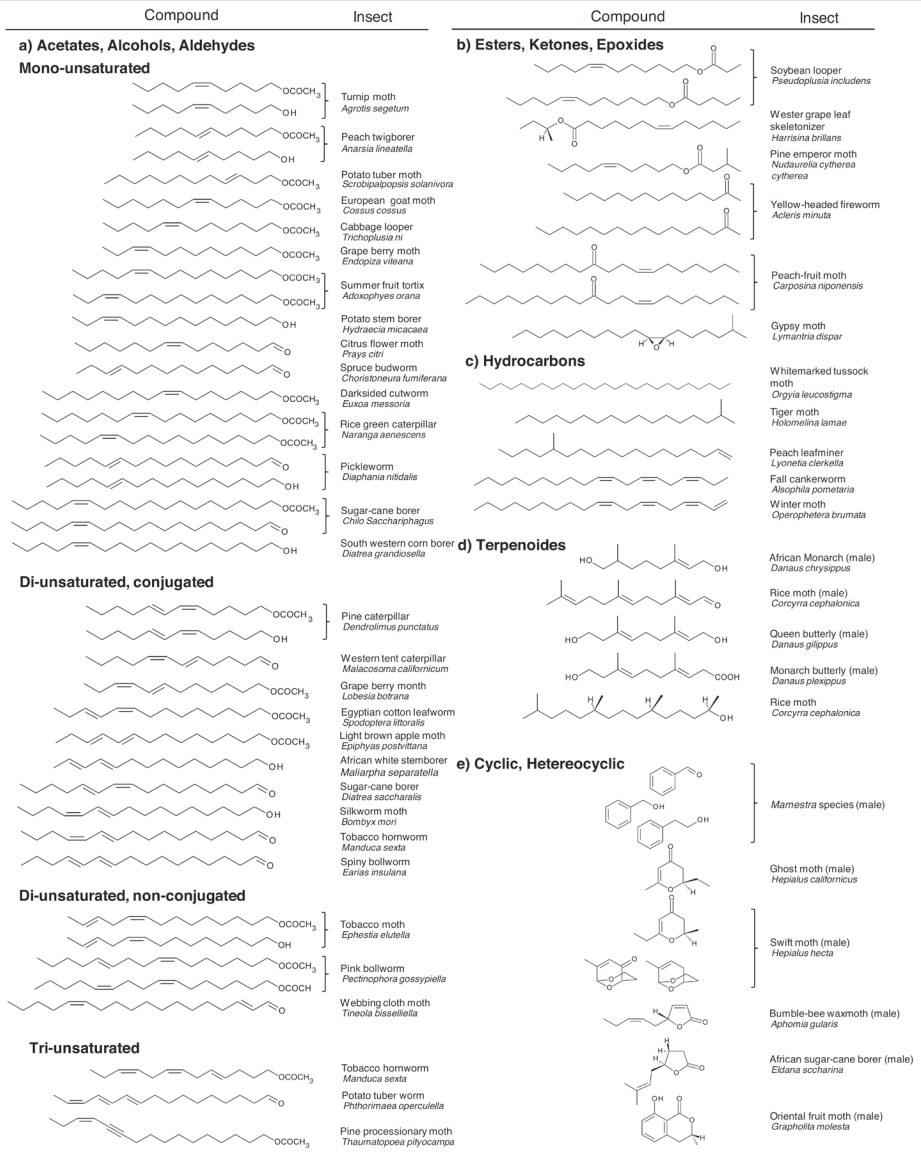

b) Collection and analyze volatiles produced by the host plant alone and by insect-colonized plants. In some instances it is also appropriate to collect volatiles from insects out of contact with the plant.

c) Locate the electrophysiologically-active components in the extract using coupled gas chromatography (GC)-electroantennogram (EAG) and coupled GC-single cell recording (SCR) techniques.

d) Identify these components using physico-chemical methods (e.g.: nuclear magnetic resonance spectrometry and coupled GC-mass spectrometry (GC-MS)) and microchemistry. Coupled GC-mass spectrometric techniques are described by Pickett.

e) Investigate the behavioral activity of these substances in laboratory and field bioassays.

f) Devise means of using the behaviorally-active substances in integrated control systems so that the use of pesticides can be minimized.

3.1. Isolation of Volatiles

An air entrainment method is employed where volatiles are captured in an air stream and collected on Porapak Q. All glassware is meticulously cleaned and heated at 200°C for several hours prior to use. Solvents are carefully purified: pentane is sequentially passed through silica gel (60-120 mesh, 200 g), activated 4A molecular sieve (50 g) and basic aluminum oxide (50 g), then distilled. Dichloromethane is freshly purified with basic aluminum oxide (90 g) before being distilled (Figure 1).

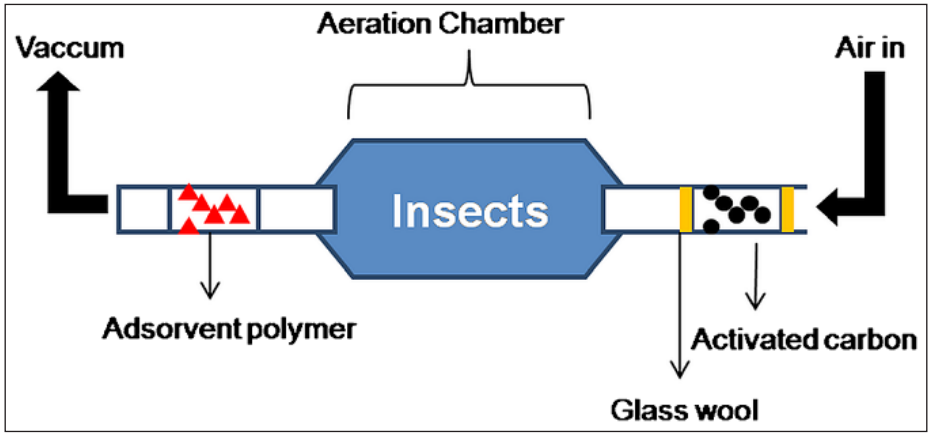

Figure 1: An aeration system used to collect insect volatiles for adsorption on a polymer

3.2. Gas Chromatography

Gas chromatography is a commonly employed technique for detecting, quantifying and characterizing volatile pheromones. Extracts of cuticular lipids from whole-body washes with solvents or volatile compounds collected from the headspace of an enclosed area are introduced into the system and column via injection or desorption, respectively. The separation of compounds occurs based on their vapor pressure and affinity for the column's stationary phase. After being eluted from the column, the compounds are typically

detected using flame ionization detection (FID) or mass spectrometry. Despite its utility in quantifying and characterizing volatile pheromones, GC has some limitations. For instance, under standard conditions used for hydrocarbon analysis, GC primarily detects low molecular weight apolar lipids. However, using high-temperature columns and adjusting temperature and ionization parameters can enable the analysis of larger molecules, such as triacylglycerides (Yew and Chung 2015).

4. Direct Analysis in Real Time Mass Spectrometry (DART-MS)

Direct Analysis in Real Time (DART) is an ionization technique that generates electronically or vibronically excited species from gases such as helium, argon or nitrogen, which then ionize atmospheric or dopant molecules. These ions interact with the sample molecules to form analyte ions. Molecules with low ionization energy may be ionized directly. The DART ionization process can produce either positive or negative ions, depending on the voltage applied to the exit electrode. In this process, the inflow gas (M) is introduced into the ion source, where an electric potential ranging from +1 to +5 kV is applied to create a glow discharge. The resulting glow discharge plasma contains short-lived energetic species, including electrons, ions and excimers. The recombination of ions and electrons have results in the formation of long-lived excited-state neutral atoms or molecules, known as metastable species (M*), in the flowing afterglow region (Figure 2).

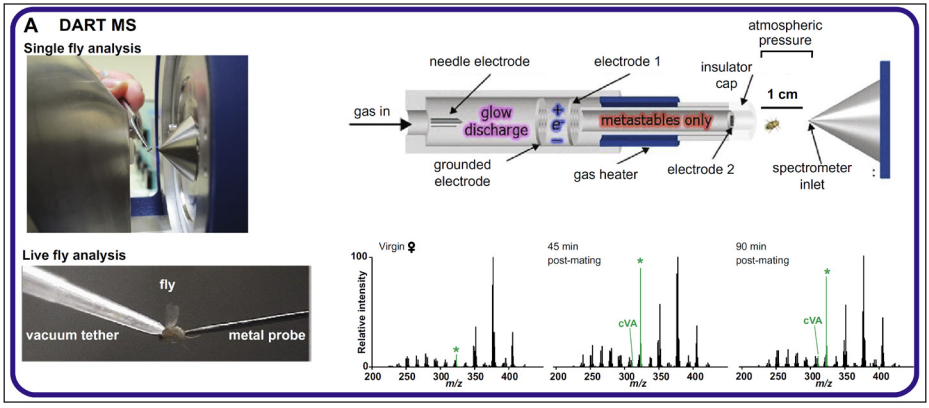

Figure 2: DART-MS, an electric potential is applied to a gas (commonly helium), creating a glow discharge that produces metastable atoms. These metastable species can desorb and ionize analytes directly from solid, liquid or gas samples. For direct analysis of insect cuticles, individual samples are positioned directly in front of the ion source and the gas stream isheated to 250-300 °C. This method also allows for the analysis of live insects by using a metal probe to sample the cuticular surface, followed by analysis of the probe. Using this approach, DART-MS spectra have shown changes in the cuticular profiles of the same fly before and after mating, with green peaks and spectra observed (Yew and Chung, 2015)

Advantages of DART-MS over other detection methods include:

a) Samples can be placed directly into an open-air ion source and require minimal preparation.

b) The source configuration accommodates a variety of sample shapes and sizes including intact insects, dissected body parts, SPME or other probes and capillary tubes dipped into liquid extracts.

c) Diagnostic capability of DART MS allows detection of more polar and higher molecular weight molecules (including, e.g., triacylglycerides, long chain fatty alcohols and sterols) that may be missed by GC-MS under standard conditions.

d) Furthermore, DART MS can directly use for the analysis of pheromone profiles from live animals in parallel with insect behavior.

glow discharge that produces metastable atoms. These metastable species can desorb and ionize analytes directly from solid, liquid or gas samples. For direct analysis of insect cuticles, individual samples are positioned directly in front of the ion source and the gas stream isheated to 250-300 °C. This method also allows for the analysis of live insects by using a metal probe to sample the cuticular surface, followed by analysis of the probe. Using this approach, DART-MS spectra have shown changes in the cuticular profiles of the same fly before and after mating, with green peaks and spectra observed (Yew and Chung, 2015).

5. Matrix-Assisted Laser Desorption/ Ionization Mass Spectrometry (MALDI)

Matrix-Assisted Laser Desorption/Ionization (MALDI) is an ionization technique that employs a laser-absorbing matrix to generate ions from large molecules with minimal fragmentation. It is particularly useful for analyzing biomolecules (such as DNA, proteins, peptides and carbohydrates) and various organic compounds (like polymers, dendrimers and other macromolecules) that are sensitive and prone to fragmentation when ionized by traditional methods (Figure 3). The matrix is composed of crystallized molecules, with the most commonly used being sinapinic acid, α-cyano-4-hydroxycinnamic acid (α-CHCA, also known as alpha-cyano or alpha-matrix) and 2,5-dihydroxybenzoic acid (DHB). MALDI is typically employed for more polar compounds. A focused laser beam, usually with a UV wavelength of 337 or 355 nm and a spot diameter of 200 μm or less, irradiates the liquid or solid sample. The sample is coated or co-crystallized with the matrix, which absorbs the laser energy and facilitates the desorption and ionization of the sample. MALDI, when used with a lithiated matrix, has been employed to analyze cuticular extracts from termites, ants, cockroaches and flesh flies, revealing unexpectedly large apolar long-chain cuticular hydrocarbons, some with more than 70 carbon atoms.

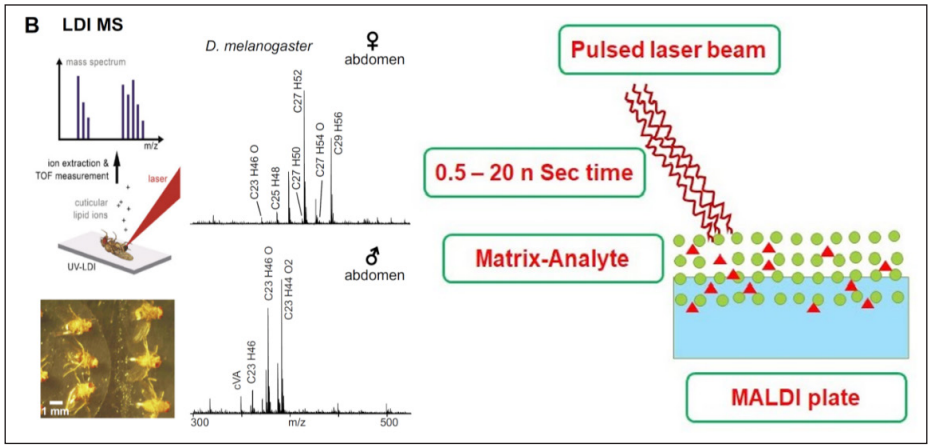

Figure 3: MALDI MS examines the surface of the insect cuticle using a laser beam with a diameter of approximately 100-200 µm, delivering high spatial resolution profiles of individual, intact insects without requiring a chemical matrix or sample extraction. An example is shown with a live *D. melanogaster* mounted on the sample plate

6. Electrospray Ionization (ESI-MS)

Mass spectrometry using electrospray ionization is referred to as electrospray ionization mass spectrometry (ESI-MS) or electrospray mass spectrometry (ES-MS). ESI is known as a 'soft ionization' technique because it causes minimal fragmentation. This is beneficial because it usually allows the detection of the molecular ion (or more precisely, a pseudo-molecular ion), though it provides limited structural information from the mass spectrum alone. This limitation can be addressed by combining ESI with tandem mass spectrometry (ESI-MS/MS). One of the main advantages of ESI is its ability to transfer solution-phase information into the gas phase. ESI was first introduced by Masamichi Yamashita and John Fenn in 1984 (Figure 4). ESI-MS can ionize a wide range of biomolecules, including both apolar and polar lipids, peptides, proteins and carbohydrates. Additionally, integrating liquid chromatography (LC) with ESI-MS can greatly improve the detection of low-abundance molecules, enhance analytical resolution and, with the use of specialized chromatography columns, aid in the identification of stereoisomers (Yew and Chung, 2015).

7. Gas Chromatography Coupled to Electroantennogram Detection (GC-EAD)

Gas chromatography coupled with electro-antennogram detection (GC-EAD) is used for the simultaneous chemical identification and quantification of functional activity. In this method, a crude extract is chromatographically separated and then divided between two detectors: part of the effluent from the GC column is directed to a flame ionization detector, while the remainder

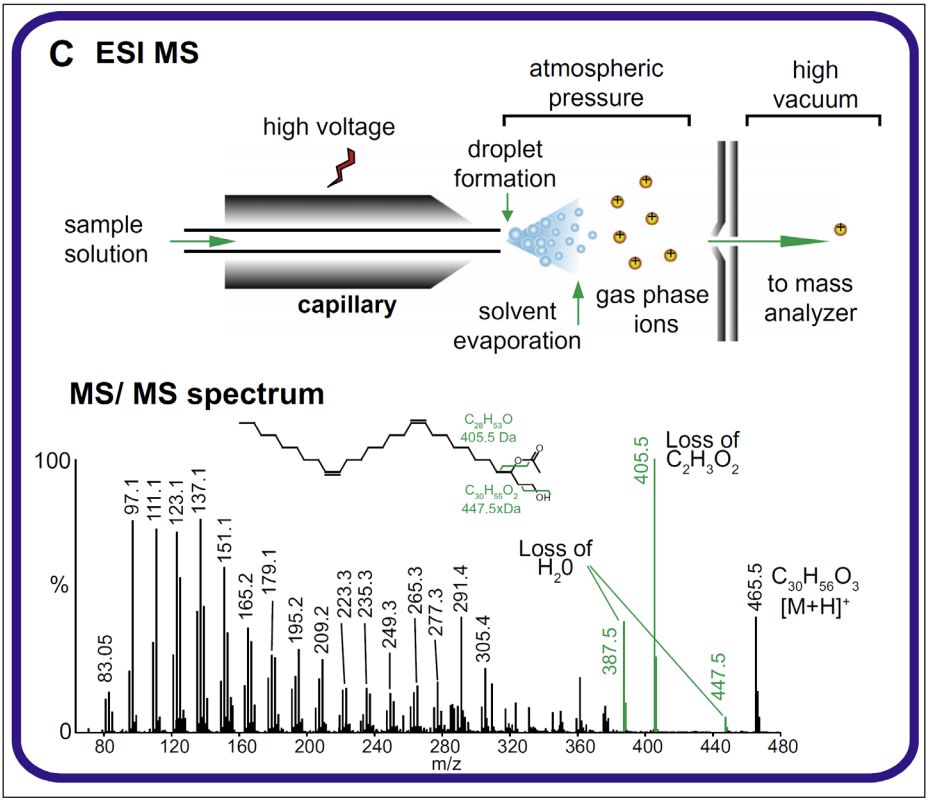

Figure 4: ESI-MS analysis, a sample dissolved in an organic solvent is introduced into a capillary. Applying a high voltage to the liquid generates a fine mist of droplets at atmospheric pressure. As the solvent evaporates and the droplets shrink, the analyte ions are released into the gas phase. The mass analyzer can select ions from a mixture based on their mass and subject them to fragmentation

is passed over a biological sensor, such as an insect. Electrodes placed in the insect's antennae or legs measure the electrical activity of sensory neurons (Figure 5). This technique has proven highly effective in identifying pheromones from various insect and arthropod species, as well as volatile odors from plants that attract insects. For instance, nonanal, an alkyl aldehyde was identified as a scent that mosquitoes use to locate humans and birds (Yew and Chung, 2015).

8. EAG Recordings

These were made using Ag-AgCI glass electrodes filled with saline but without glucose. The recording electrode is positioned in the distal end of the antenna and the indifferent electrode at the base.

Recent years several light weight prototypes were developed for rapid and

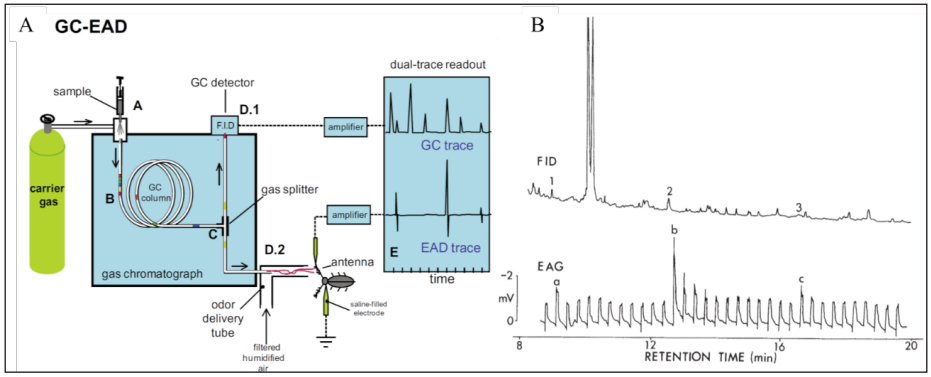

Figure 5: (A) GC-EAD, a crude extract is separated on a GC column and the resulting sample stream is directed to both a mass detector and an insect electroantennogram setup. Compounds that trigger a positive electrical response are considered potential chemical communication signals (Yew and Chung, 2015); (B) A typical GC-EAG analysis of solvent-extracted female moth volatiles captured on charcoal is shown. The top trace represents the gas chromatogram obtained from the flame ionization detector. GC conditions include using a polar CP Wax 52CB fused silica capillary column, with the temperature initially set at 70 °C, then increasing at 20 °C/min to 120°C, followed by a rate of 4 °C/min to 210 °C, with helium as the carrier gas (0.6 kg/cm²) (McCaffery and Wilson, 1990)

filed identification insect VOCs such as Pawson *et al.* (2020) developed a lightweight device for *Lymantria dispar dispar* containing dual signal electrodes and a central reference electrode (Figure 6(F)). This new device is light weight (516 g) and more compact (12 × 12 × 8 cm, with a volume of 1152 cm³) compared to previous models. It can accommodate insects with antennal lengths ranging from 4 to 30 mm, offers wireless communication with a range of 600 m in urban settings and up to 10 km in line-of-sight conditions, has a standalone power supply and utilizes both antennae of the test insect. The device showed normalized antennal responses for *Epiphyas postvittana* in a dose-response experiment, where its performance was comparable to traditional laboratory EAG equipment. In dose-response tests, the mean detection limits for pheromone sources were 100 ng for *E. postvittana*, 100 ng for *Agrotis ipsilon* and 1 ng for *L. dispar dispar*.

9. Single-Cell Recordings (SCR)

These were obtained from individual olfactory cells using tungsten microelectrodes. For aphids, the indifferent electrode is positioned in the first antennal segment, while for Coleoptera, it is placed in the scape or mouthparts. The recording electrode is then positioned on the surface of the antenna until impulses are detected (McCaffery and Wilson, 1990) (Figure 7).

Li *et al.* (2021) developed an EGA techniques to detect volatile organic compounds (VOCs) using the antennal lamellae of a Scarab beetle

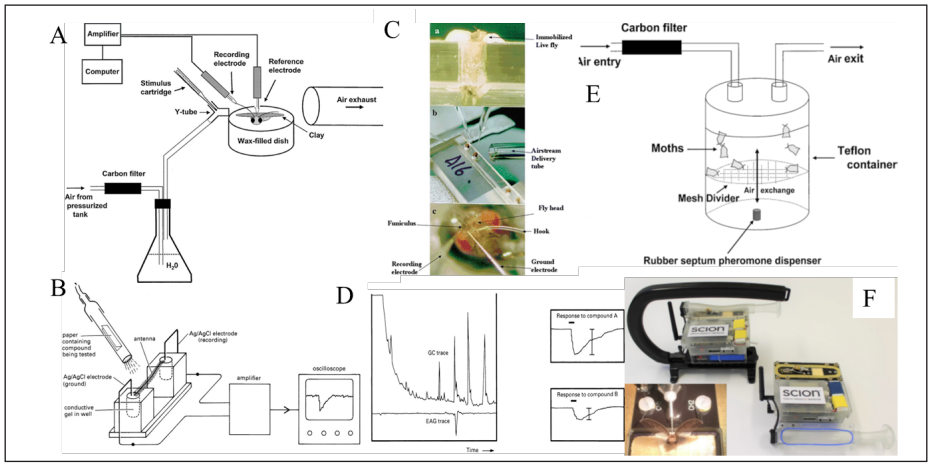

Figure 6: A) Design of the electroantennogram recording and stimulus delivery system (Lukasz *et al.*, 2003); B) Single antenna EAG setup; D) Reading the antennogram; E) Adaptation chamber: a 1-liter Teflon container with glass inlet and outlet, featuring a wire mesh divider that prevents insects from contacting the pheromone dispenser while allowing air exchange at a flow rate of 30 ml/min (Lukasz *et al.*, 2003); F) Portable device for detecting insect volatile compounds, shown with the airflow tube removed in the lower image and a unit mounted for handheld use. The insert shows *Lymantria dispar dispar* connected to the dual signal electrodes and central reference electrode of the pEAG (Pawson *et al.*, 2020)

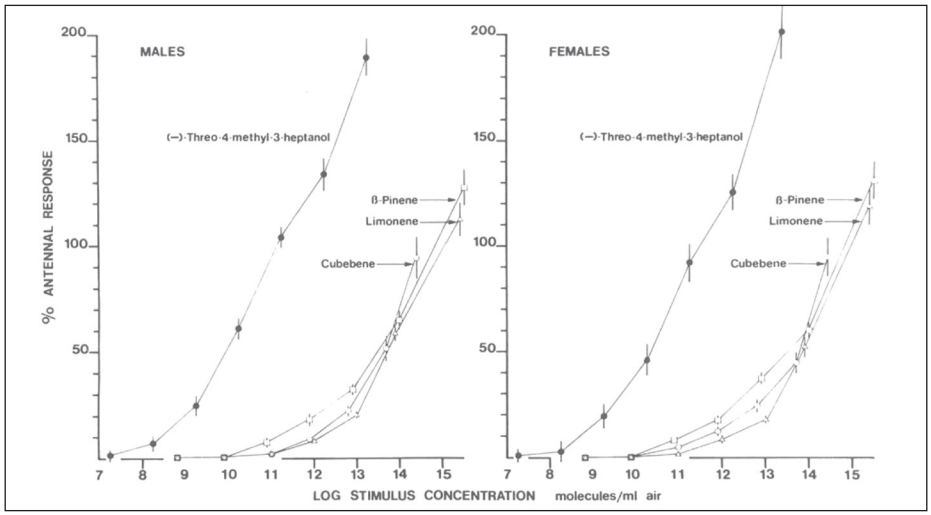

Figure 7: EAG responses of male and female *S. scolytus* to (-)-threo-4-methyl-3-heptanol, (-)-α-cubebene, (-)-β-plnene and limonene. Responses arenormalized with respect to a (±}-threo-4-methyl-3-heptanol (McCaffery and Wilson, 1990)

(Pseudosymmachia flavescens). The EGA setup included a 5-arm olfactometer and utilized six different plant volatiles: Anisole (99%), Z-3-hexenal (50% in triacetin, stabilized), eucalyptol (99%), 6-methyl-5-hepten-2-one (99%), 1-hexanol (98%), (-)-E-pinocarveol (96%) and 4-ethyl-phenol (99%). The results indicated that test stimuli produced similar EAG depolarization profiles across the three lamellae and the closed club, although the EAG amplitudes varied significantly among different chemical stimuli. The mid lamella generally generated notably stronger EAG responses. EAG responses to the sex pheromone component anisole were significantly correlated with the density of sensilla placodea subtype 1 (SP1). Anisole elicited significantly stronger responses in males, ranging from 1.77-2.83 mV at 0.1 mg and 3.21-4.27 mV at 1.0 mg, demonstrating a sex-specific response pattern (Figure 8).

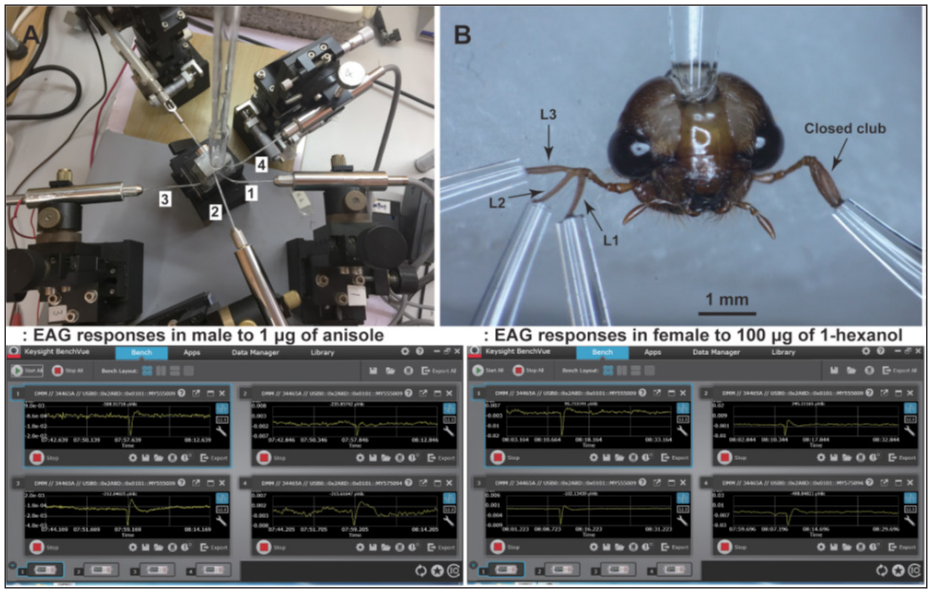

Figure 8: Experimental setup (A) and antennal preparation (B) for EAG recordings are depicted as follows: The head of a beetle is isolated and placed on a dental wax stage. The reference electrode is attached to the neck, while the recording electrodes are connected to the three distinct lamellae, L1, L2 and L3, of one antennal club, as well as to the other closed club. The recording electrodes are labeled 1, 2, 3 and 4, corresponding to lamellae L1, L2, L3 and one antennal club, respectively (Li *et al.*, 2021)

10. Nuclear Magnetic Resonance Spectroscopy (NMR)

Nuclear Magnetic Resonance (NMR) is a physical phenomenon where nuclei within a strong, constant magnetic field are disturbed by a weaker, oscillating magnetic field. This disturbance causes the nuclei to emit an electromagnetic signal at a frequency that reflects the magnetic field at the nucleus. This effect is observed near resonance, which occurs when the frequency of the

oscillating field aligns with the natural frequency of the nuclei. This natural frequency is influenced by the strength of the static magnetic field, the chemical environment and the magnetic properties of the specific isotope. In practical use, this resonance is typically achieved with static magnetic fields of up to about 20 tesla.

Nuclear Magnetic Resonance (NMR) is considered the gold standard for precise structural elucidation. However, it typically requires several hundred micrograms to milligrams of pure substance for analysis, which can be difficult for low-abundance molecules isolated from natural sources. Recent advancements in detection sensitivity and spectral interpretation techniques have made NMR a valuable tool for screening signaling molecules in complex mixtures. Additionally, differential analysis of 2D NMR spectra enables comparison of spectra from different conditions, as demonstrated in the successful identification of attractant pheromones from *Caenorhabditis elegans* by comparing active and inactive fractions. Despite its advanced capabilities, NMR has limitations, such as the time-consuming and challenging manual interpretation of spectra. Automated computational methods driven by AI are becoming essential for efficiently analyzing complex biological compounds (Figure 9).

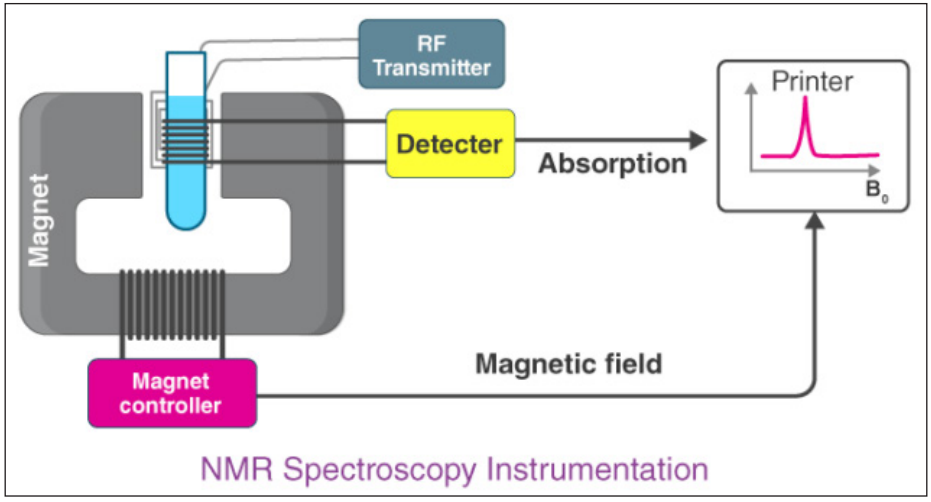

Figure 9: The configuration of an NMR setup involves aligning the magnetic nuclear spins within a constant magnetic field, denoted as B0. This alignment is then disturbed by a weak oscillating magnetic field, commonly known as a radio frequency (RF) pulse. The frequency of this RF pulse needed to cause significant perturbation depends on both the strength of the static magnetic field (B0) and the specific nuclei being observed. The NMR signal is detected either during or after the RF pulse through the voltage induced in a detection coil by the precession of the nuclear spins around B0. Following an RF pulse, the nuclei typically precess at their Larmor frequency, a process that does not involve transitions between spin states or energy levels.

11. Biosensors

The cuticular wall of an olfactory sensillum features numerous pores that allow odor molecules from the environment to enter the olfactory system. For these hydrophobic odorants to interact with olfactory receptors (ORs) and OR co-receptor (Orco) ion channels on the sensory dendrites of olfactory neurons, they first need to be solubilized and transported by odorant binding proteins (OBPs). OBPs are extracellular proteins secreted by the supporting cells surrounding olfactory neurons and are found in high concentrations in the surrounding lymph. A biosensor is a device that detects biological or chemical reactions by producing signals proportional to the concentration of an analyte in the reaction. To replicate the sense of smell, researchers have developed novel artificial olfaction systems in vitro, known as smell or olfactory biosensors (see Table 3). These biosensors are analytical tools that integrate biological or bio-derived sensitive components with various physicochemical transducers to detect target analytes (Figure 10). Utilizing Micro-Electro-Mechanical Systems (MEMS) and nanotechnology, olfactory biosensors have been created for applications in environmental monitoring, food quality control and clinical diagnostics (Lu and Liu 2022).

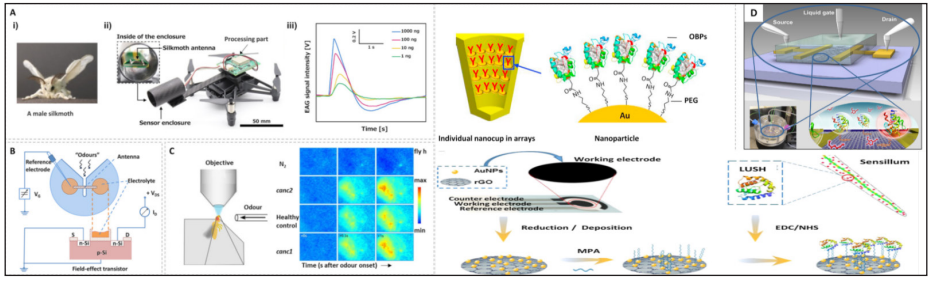

Figure 10: OBP-based electrochemical biosensors include several key components and techniques. (A) The schematic diagram shows an interdigitated electrode device used for impedance measurement. (B) It illustrates impedance spectra for varying concentrations of isoamyl acetate. (C) The structure of odorant binding proteins (OBPs) from the oriental fruit fly (*Bactrocera dorsalis*) and the binding interaction between an OBP and isoamyl acetate are depicted. Additionally, there are odorant binding protein-based localized surface plasmon resonance biosensors and field-effect transistor biosensors. (A) This schematic diagram features nanocup arrays functionalized with self-assembled OBPs (Source: Lu and Liu, 2022)

Antenna-based biosensors have primarily been developed using electroantennography, a technique that measures the average electrical response of an insect's antenna to various odorants. These biosensors are designed to capture, preserve and integrate data with various types of sensors, including field-effect transistors (FETs), electrochemical impedance spectroscopy (EIS) sensors and surface plasmon resonance (SPR) sensors. Commonly used proteins in these biosensors include olfactory receptors

(ORs), odorant binding proteins (OBPs) and peptide sequences derived from olfactory proteins.

Table 3: Olfactory biosensors based on insect Electroantennogram (EAG)

Measurement techniques	Insect species	Target molecule	Detection range	Detection limit
Electro-antennogram (EAG)	*Calliphora vicina* (blowfly)	1,4-Diamino-butane	4.4 ng-44 µg	1 ng
	Leptinotarsa	(Z)-3-Hexen-1-ol, (E)-2-hexenal and linalool	10 pg-100 ng	1 pg
	Decemline-ata, Calliphora vicina	1,4-Diamin-obutane, 1-hexanol, butanoic acid	1 ppb-100 ppm (1,4-diamino-butane); 20-200 ppm (1-hexanol); 8-500 ppm (butanoic acid)	-
	Drosophila melanogaster	cis-11-Hexa-decenal, cis-3-hexenol, hexanoic acid, benzyl acetate, 2-methyl-5-nitroaniline, cyclohexanone	-	-
	Heliothis virescens	α-pinene, cisnerolidol	-	-
	Helicoverpa zea	trans-nerolidol, β-caryophyllene, β-ocimene	-	-
	Ostrinia nubilalis	(R)-(+)-limonene, methyl jasmonate	-	-
	Microplitis croceipes	2-diisopropyl amino ethanol, indole, 2,2-thiodiethanol,	-	-
		1-heptanol, 1-octanol, 1-nonanol, 1-decanol		

Measure-ment techniques	Insect species	Target molecule	Detection range	Detecti-on limit
Electro-antenno-gram (EAG)	*Helicoverpa zea,* Male *Anticarsia gemmatalis, male Trichoplusiani, male Heliothis virescens,* male *Helicoverpa zea*	Z-11-Hexadecenal, Z-11-Hexadecenal, Z-11-tetradecenyl acetate, E,E-8,10-dodecadien-1-ol, E-11-tetradecen-1-ol	1-100 µg 100 µg	1 µg
	Agrotisipsilon	Z-7-Dodecenyl acetate	1 µg, 10 µg	-
	Bombyx mori	Bombykol	1-1000 ng	-
Field-effect transistor (FET)	*Leptinotarsa decemlineata*	cis-3-Hexen-1-ol	1 ppb-100 ppm (cis-3-hexen-1-ol), 5-500 ppb (guaiacol)	1 ppb (cis-3-hexen-1-ol), 100 ppb (guaiacol, 1-octen)
	Leptinotarsa decemlineata	cis-3-Hexen-1-ol, guaiacol, 1-octen	1-100 ppt (cis-3-hexen-1-ol)	1 ppt (cis-3-hexen-1-ol)
	Phaenops cyanea	cis-3-Hexen-1-ol, guaiacol	-	-
Fluore-scence	*Drosophila melanogaster*	Volatile organic compounds of cancer cells	-	-

12. Odorant Binding Protein-based Biosensors

To detect odors, hydrophobic odorant molecules must first be solubilized and transported from the lymph of chemosensilla to the membranes of olfactory receptor neurons. The odorant binding protein (OBP) family comprises two types: pheromone binding proteins (PBPs) and general odorant binding proteins (GOBPs). Unlike membrane proteins such as olfactory receptors (ORs), OBPs are smaller, globular proteins with a molecular weight of approximately 10-30 kDa, making them easier to isolate and purify. Additionally, OBPs are known to be stable across a wide range of pH and

temperatures (up to 80°C), maintaining their binding properties even under harsh conditions (Table 4). Different olfactory biosensors using OBPs from honeybees (*Apis cerana cerana*) and oriental fruit flies (*Bactrocera dorsalis*) have been developed with interdigitated electrodes. The data from these sensors are analyzed using the Randles circuit model, which includes four components: solution resistance (Rs), charge transfer resistance (Rct), Warburg impedance (Zw) and constant phase element (CPE). Typically, Rct is used as the primary parameter for interpreting protein-ligand interactions (Lu and Liu, 2022).

Table 4: Insect odorant binding protein-based biosensors

Measurement techniques	**Biosensing elements**	**Target substances**	**Detection range**
Electrochemical impedance spectroscopy (EIS)	OBPs from honeybee (*Apis cerana cerana*)	Linalool, geraniol, β-ionone, 4-allylveratrole, phenylacetaldehyde, dibutyl phthalate, isoamyl acetate, methy-p-hydroxyl benzoate	$10\text{-}6\text{-}10^{-3}$ M
	OBPs from honeybee (*Apis cerana cerana*)	Isoamyl acetate	$10^{-9}\text{-}10^{-4}$ M
	OBPs from oriental fruit fly *(Bactrocera dorsalis*)	Isoamyl acetate, β-ionone, benzaldehyde	$10^{-7}\text{-}10^{-4}$ M
	OBPs from oriental fruit fly (*Bactrocera dorsalis*)	Benzaldehyde	$10^{-7}\text{-}10^{-3}$ M
	CSPs from honeybee (*Apis cerana cerana*)	Isoamyl acetate, geraniol, phenylacetaldehyde	$10^{-7}\text{-}10^{-4}$ M
	OBPs from fruit fly (*Drosophila melanogaster*)	Denatonium, quinine, berberine	$10^{-9}\text{-}10\text{-}6$ mg mL^{-1}
	OBPs from honeybee (*Apis cerana cerana*)	Methyl p-hydroxy-benzoate, vanillyl alcohol	$10^{-7}\text{-}10^{-4}$ M
Localized surface plasmon resonance (LSPR)	OBPs from honeybee (*Apis cerana cerana*)	β-Ionone, 2,4,6-trinitrotoluene (TNT), 2,4-Dinitrotoluene (DNT)	0.01^{-1} mM

Measurement techniques	Biosensing elements	Target substances	Detection range
Field-effect transistor (FET)	OBP 14 from honeybee (*Apis mellifera*)	Homovanillic acid, methyl vanillate, eugenol, citral, methyl eugenol, geraniol	0.1-200 µM
	OBP14 from honeybee (*Apis mellifera*)	Homovanillic acid	0.1-100 µM
	OBP14 from honeybee (*Apis mellifera*)	Eugenol, homovanillic acid	0.1-200 µM
	OBPs from fruit fly (*Drosophila*), LUSH	Eugenol, homovanillic acid	0.001-1%

13. Wind Tunnels and Olfactometers Bioassays

Wind tunnel experiments have been valuable for investigating the physiological and behavioral limits imposed by various plume strengths and structures on male insects' olfactory systems. These tests help identify attractive or repellent odors, insect flight patterns, visual-odor interactions and the effects of background odors in the environment. Using a wind tunnel allows researchers to study insect odor-mediated behaviors in a controlled laboratory setting (Figure 12). Behavioral observations under

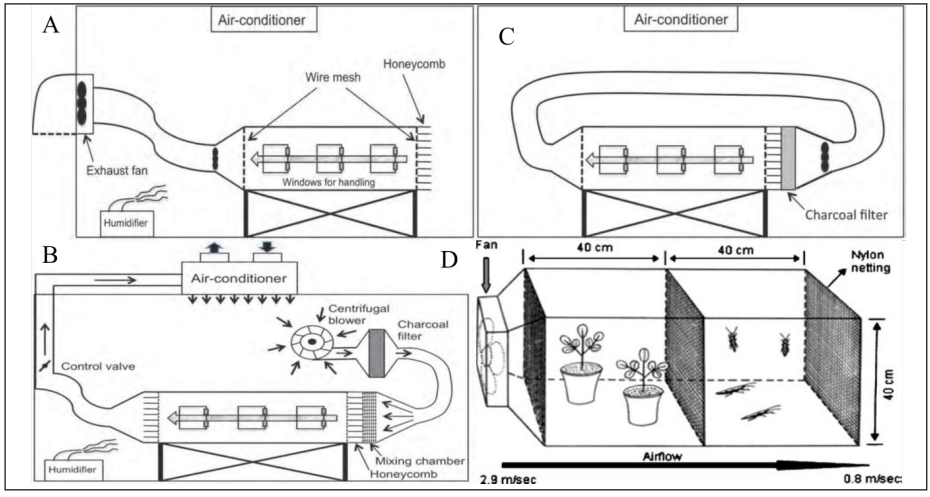

Figure 12: Various wind tunnel configurations are available for behavioral studies include: (A) pulling-air type wind tunnels, (B) pushing-air type wind tunnels designed for air recycling, (C) wind tunnels that combine both pushing and pulling air types and (D) setups where moths are exposed to odors from non-host pea plants within the wind tunnel (Zhang *et al.*, 2007; Kainoh, 2011)

these controlled conditions help link insect physiology, migration patterns and field applications. Wind speed plays a crucial role in these experiments, with most studies finding an optimal speed of 25 to 30 cm/sec. According to Kainoh *et al.* (1984), wind speeds between 30 and 60 cm/sec are effective for testing the sex pheromone of *Adoxophyes honmai* (Lepidoptera: Tortricidae), although some insects require lower wind speeds, around 25 to 30 cm/sec (Kainoh, 2011).

14. Olfactometer Assays

Obermayr *et al.* (2012) designed a Y-Tube Olfactometer assay system featuring a transparent Plexiglas base leg, a decision chamber and two branches that end in Teflon chambers where test stimuli are introduced (Figure). Air from a pressurized system was purified through an activated charcoal filter, heated to 26±1 °C and humidified to a relative humidity of 70±5% before being channeled through the apparatus. The wind velocities were set at 0.4 m/s in the branches and 0.2 m/s in the base leg. Rotating doors in both branches and at the downwind end of the base leg facilitated the release and capture of test mosquitoes. Groups of 15-21 mosquitoes were introduced into the apparatus at its downwind end. The Y-Tube Olfactometer, as described by Geier and Boeckh (1999), includes: Cage 1 (release chamber) for the test mosquitoes, a decision chamber where mosquitoes choose between the two branches and Cages 2 and 3 (test and control cages) where volatile stimuli and pure air are applied, respectively. The apparatus, including grid and rotating doors made of mesh gauze, has a total length of 105 cm.

A variety of Y-tube olfactometers are available online, including the vertical Y-tube olfactometer (VYTO) developed by Das in 2021. This three-armed VYTO was designed based on the observation of the pest's negative geotactic crawling movement (NGCM) in a circular pattern within a closed cylindrical chamber. The VYTO, with some modifications from Patt and Setamou (2010) and Coffey *et al.* (2016), was constructed following the World Health Organization's guidelines for Y-tube olfactometers and spatial repellent assays (WHO, 2013). The VYTO was built at the Glass Blowing Centre of Tezpur University (Figure 13 (A)). It features a Y-shaped glass tube with an internal diameter of 3.5 cm and a thickness of 0.18 mm, with each arm measuring 40 cm in length and comprising a test chamber, treated chamber and control chamber. The treated and control chambers are positioned at a 45° angle to each other, allowing the pest to choose between two odor fields. To facilitate the pest's crawling movement and ensure clear observation during the bioassay, the internal surfaces of all three chambers are lined with white chart paper. For the adjustable external components, namely A, B and C (Figure 13 (B)), each 500 ml round-bottom flask (Borosil) was connected to a glass regulator (internal diameter: 3.5 cm, thickness: 0.18 mm) to manage the air supply. These adjustable parts were designed to fit securely with the main Y-tube body and the open ends of the glass regulators were attached to flexible rubber tubes (diameter: 0.5 mm), which were then connected to a vacuum pump (Tarson: Model No-410) for controlled

air cleaning and supply. The entire setup was vertically mounted using a custom wooden frame (Das, 2021).

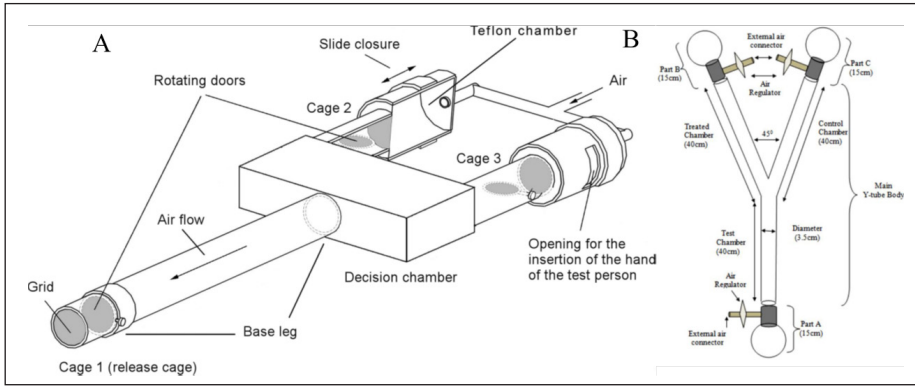

Figure 13: Configuration of olfactometer developed by Geier and Boeckh (1999) and Das (2021)

15. Pheromone Dispensing Technology/ Pheromone Release Systems

The first pheromone for pest monitoring was registered in the 1970s. During the 1980s and 1990s, pheromones were introduced for mating disruption in vineyards orchards and fields of tomatoes, rice and cotton. In typical mating disruption setups for vineyards, approximately 500 pheromone dispensers are placed per hectare at the start of the first generation's flight period, with one dispenser every 20 m^2. Each dispenser contains 438 mg of pheromone compounds, including 205 mg of (Z)-9 dodecenyl acetate and 233 mg of (E/Z)-7,9 dodecadienyl acetate. Under optimal conditions, a single dispenser can disrupt mating for 150-180 days, which implies a theoretical release rate of about 3 mg per day per dispenser or 1.5 g per hectare per day. In contrast, field studies for mass trapping of oriental fruit moths have identified an optimal concentration range in upwind conditions between approximately 7×10^{-17} and 2×10^{-13} g/cm^3, equivalent to 7×10^{-7} and 2×10^{-3} g/ha (assuming a vertical dimension of 1 meter: 100 × 100 × 1 m^3 per hectare).

Traditional pheromone release systems include laminate dispensers, waxy dispersions and various polymer-based formats such as flakes and chips. However, microencapsulation has become a prominent formulation method for mating disruption (Figure 14). In these microparticle systems, a highly concentrated pheromone is enclosed in an inner core, which is then covered by an outer shell designed with specific diffusion properties (Hellmann *et al.*, 2023).

The release rate of polyurethane (PU) and polyamide (PA) capsules, which vary in diameter from 2 to 10 µm, is affected by the diffusion parameters of the capsule walls, which are influenced by the level of chemical cross-linking (see Table 5). In laboratory conditions with no wind, cross-linked PU/PA capsules exhibited a slow release rate, reaching approximately 20%

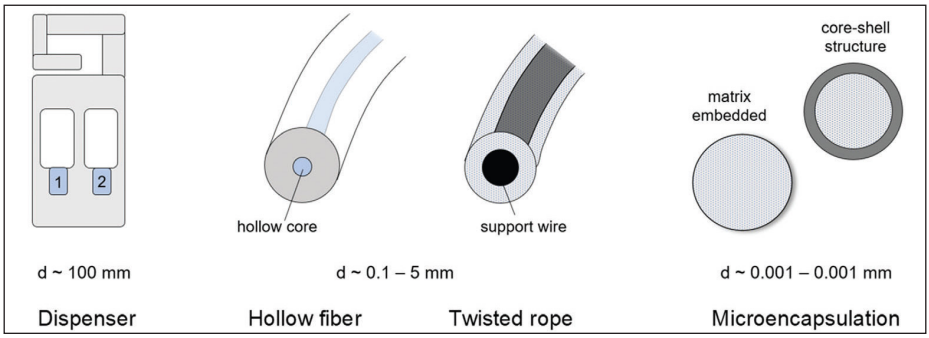

Figure 14: Pheromone release systems (pheromone indicated in light blue, d = diameter)

after about 3 weeks. However, in field trials, about 80% of the pheromone was released within 1 week (Figure 15). Formulations using paraffin wax and soybean oil demonstrate zero-order release kinetics, with release rates of around 2 mg per day for 40 days. For effective disruption of mating in European grapevine moths and vine moths in vineyards, a release rate approximately 50% higher (1.5 g per hectare per day) is required from a point source (Hellmann *et al.*, 2023).

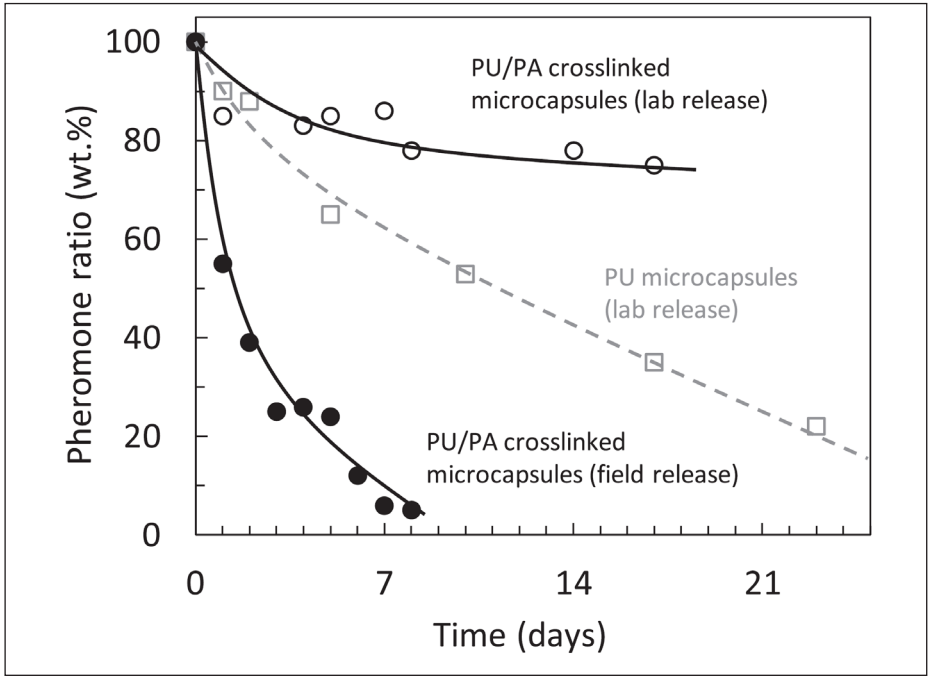

Figure 15: The release behavior of cross-linked microparticles made from polyurethane (PU) and polyurethane/polyamide (PU/PA) was studied under both laboratory and field conditions (Hellmann *et al.*, 2011)

16. Polymer Carriers

Pheromones released from these matrices generally disrupt male mating behavior through one of three main mechanisms (Hellmann *et al.*, 2023):

i) They compete with potential mates, causing males to expend time and energy approaching the pheromone sources instead of locating females.

ii) They induce sensory impairment, diminishing or completely inhibiting the males' ability to detect female pheromone trails.

iii) They generate disruptive pheromone "noise" that obscures the pheromone signals of calling females.

The transport characteristics of pheromones released from polymer matrices are mainly explained by Hendry's and Fick's laws. Key factors influencing transport in specific active substance and polymer systems include (Hellmann *et al.*, 2023):

i) The concentration of the pheromone in the reservoir.

ii) The thickness of the barrier, assuming that the energy of free rotation, free volume and intermolecular interactions remain constant.

iii) Factors affecting transport properties are illustrated in (Figure 16).

Table 5: Some recent development of polymer carrier in pheromone technology

Sl. No.	Culture/ Insect species	Dispenser type/ Formulation	Polymer	Pheromone
1	Pinkbollworm (*Pectinophora gossypiella*)	Hollow fibers, twisted rope, microen-capsulation	Poly (ethylene)	(Z,Z)- and (Z,E)-7,11-hexadecadienyl acetates
2	Apples/ codling moth (*Cydia (Laspeyresia) pomonella*)	Hollow fibers, flakes, tube dispensers	Poly (ethylene)	(E,E)-8,10-dodecadien-1-ol, dodecan-1-ol, tetradecan-1-ol
3	Apples/ light brown apple moth (*Epiphyas postvittana*)	Twisted rope dispensers	Poly (ethylene)	(E)-11-tetradecenyl acetate (E,E)-9,11-tetradecadienyl acetates (20:1)
4	Stone fruits/ oriental fruit moth (*Grapholita molesta*)	Tube dispensers	Poly (ethylene)	(Z)-8-dodecenyl acetate, (E)-8-dodecenylacetate, 95:5 (Z) to (E) acetate, including 3-10% (Z)-8-dodecen-1-ol

Sl. No.	Culture/ Insect species	Dispenser type/ Formulation	Polymer	Pheromone
5	Black currants/ currant clearwing moth (*Synanthedon tipuliformis*)	Twisted rope dispensers	Poly (ethylene)	(E,Z)-2, 13octadecadienyl acetate, (E,Z)-3, 13-octadecadienyl acetate (100:3)
6	Tomato pinworm (*Keiferia lycopersicella*)	Hollow fibers	Poly (ethylene)	(E)-4-tridecenyl acetate, (Z)-4-tridecenyl acetate 96:4
7	European grape moths *Eupoecilia ambiguella, Lobesia botrana*	Tube dispensers	Poly (ethylene)	(Z)-9-dodecenyl acetate, (E,Z)-7,9-dodecadienyl acetate (1:1.1)
8	North American grape moths *Endopiza* (= *Paralobesia*)	Twisted rope dispensers	Poly (ethylene)	(Z)-9-dodecenyl acetate, (Z)-11-tetradecenyl acetates (9:1)

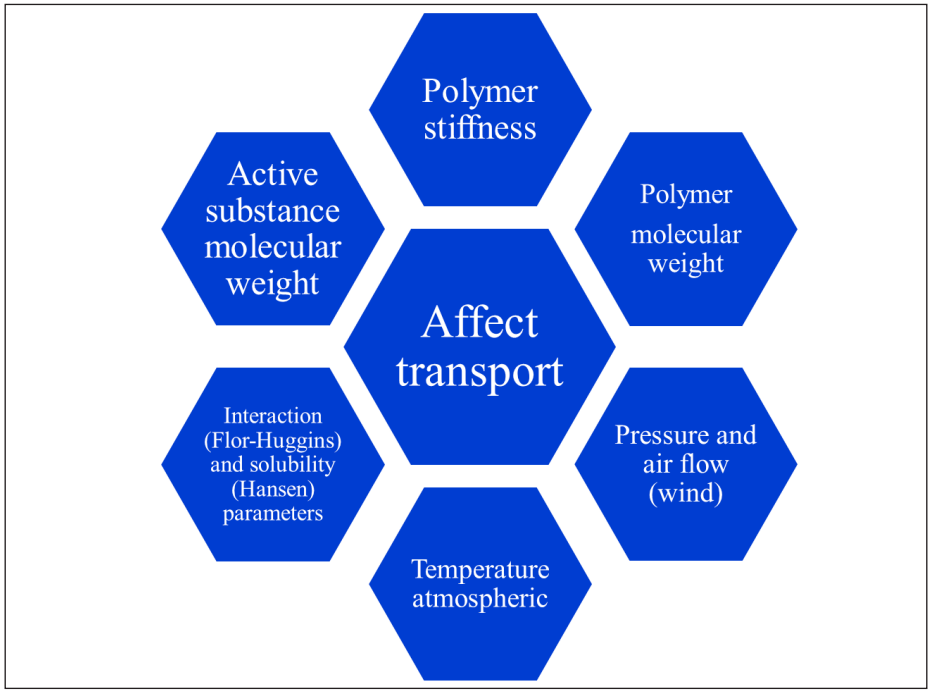

Figure 16: Affect transport properties of pheromone after deployments (Hellmann *et al.*, 2023)

Most controlled-release methods operate based on zero-order kinetics, where the release rate remains constant over time. This equilibrium release kinetics typically occurs at the initial stage in reservoir-barrier systems due to the high initial pheromone concentration in the reservoir and the diffusion being influenced by the barrier thickness. As the pheromone concentration in the reservoir declines, the system shifts to first-order release kinetics, characterized by a decreasing release rate over time (Figure 17). The release characteristics are also affected by the choice of system, such as multi-dosage fast-release systems, diffusion-controlled release systems and heterogeneous, externally-induced release systems (Hellmann *et al.*, 2023).

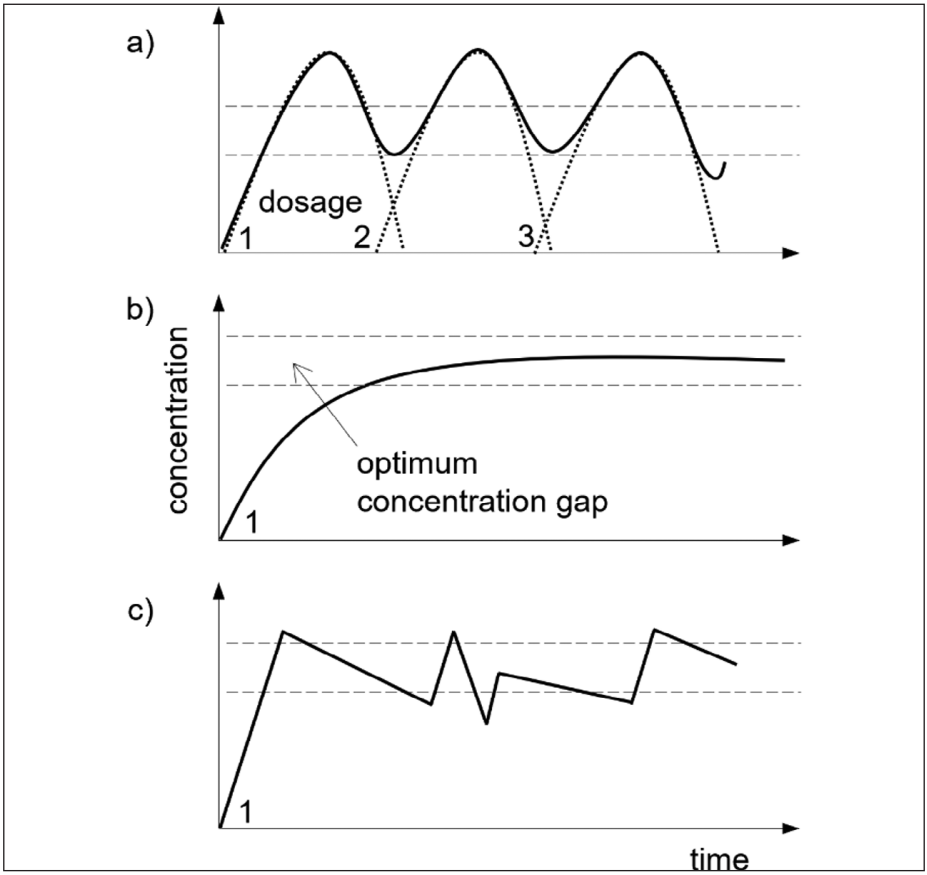

Figure 17: The concentration of pheromones over time depends on the release mechanisms used: a) Cumulative concentration resulting from the application of individual doses, b) Controlled release from a single dose over an extended period, c) Responsive release mechanisms, where varying release characteristics over time can be adjusted by activating the release of additional active substances through stimuli such as light, heat or magnetic pulses (Hellmann *et al.*, 2023)

17. Disadvantages of Conventional Pheromone Dispensers

i) Point sources can cause the pheromone concentration to drop below the minimum level needed for effective mating disruption when measured several meters away.

ii) As a result, the pheromone concentration near the dispenser is much higher than necessary, ensuring that the minimal effective concentration is maintained halfway to the next point source.

iii) Sprayed pheromone formulations often release the pheromones too rapidly in field conditions.

18. Modern Generation of Pheromone Dispensers

Alternative fine fibrous dispenser systems, resembling spider webs, have been explored to overcome the limitations of sprayed formulations. These continuous fine fibers can be evenly spread across fields using specialized machinery, adhere to plants without obstructing their growth or light access and are durable against wind and rain. The pheromone dispensing technologies include the Pheromone Nanogel Technique and microencapsulated pheromone technology (Figure 18 and 19). Various fiber materials, including Polyamide 6 (PA6), biodegradable cellulose acetate (CA) and biodegradable polyester, were tested to optimize the uptake and release of (E,Z)-7,9-dodecadienyl acetate. The CA/acetone spinning solution achieved a maximum pheromone load of approximately 29% (w/w) with an 86% yield, releasing about 57% of the pheromone over 8 weeks in a nearly linear pattern (Baker and Roelofs, 1981). The polyester/chloroform spinning solution also reached a maximum pheromone load of around 29% (w/w) with an 88% yield. These polyester fibers released approximately 25% of the pheromone over nearly 8 weeks with near zero-order kinetics (release rate ≈0.1% (w/w) per day). Field tests with pheromone/polyester fibers showed effective mating disruption lasting 3 weeks (Greiner and Wendorff, 2007). These tests involved using about 450 meters of hail protection nets coated with fibrous pheromone carriers, with segments approximately 1.5 meters in length distributed evenly over a vineyard area of around 2000 m².

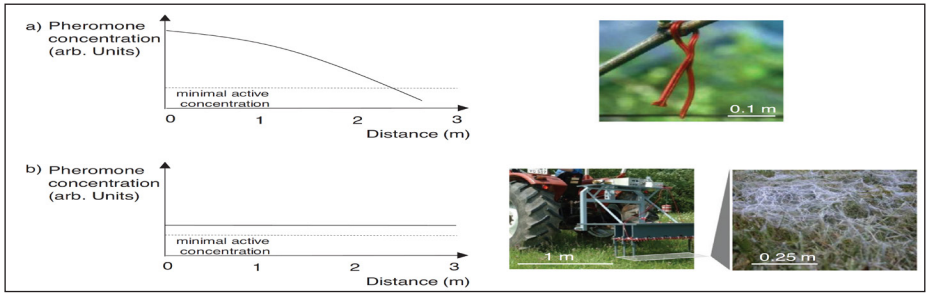

Figure 18: The typical release profile of a common pheromone dispenser-type point source

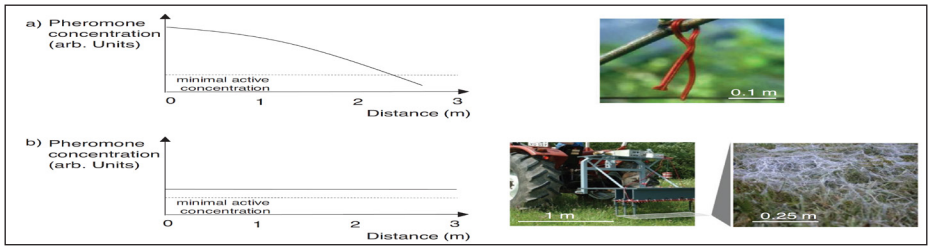

Figure 19: The use of fine fibers as potential pheromone carrier systems, which are manufactured directly in the field, has been explored (Greiner and Wendorff, 2007)

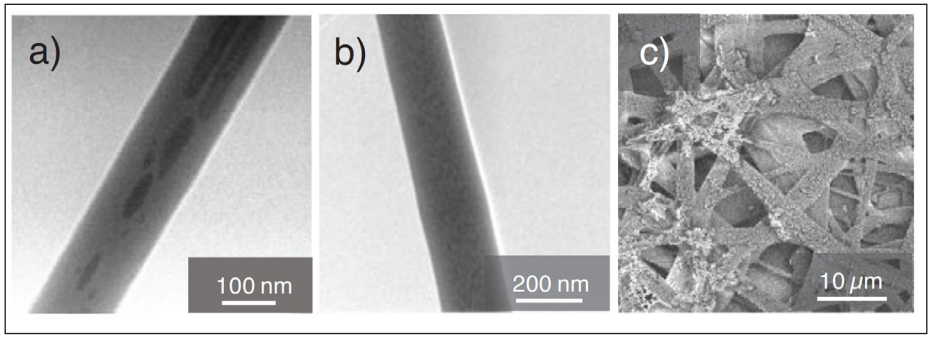

Figure 20: Pheromone-loadedfibers. TEM images of pheromone-loaded: (a) polyamide 6 (PA6); (b) cellulose acetate (CA) fibers after staining with ruthenium tetroxide; (c) Pheromone-loaded polyester fibers

19. Metal-Organic Frameworks (MOF)

Metal-organic frameworks (MOFs), also known as porous coordination polymers (PCPs), represent a notable category within coordination chemistry. These materials are characterized by their coordination networks, which contain potential voids. MOFs are constructed from organic linkers that extend periodically through metal nodes, forming a sophisticated class of porous materials that have experienced significant growth and interest in recent decades (Ghosh, 2019). MOFs are defined by their porous structures created through coordinative bonding between metal ions and organic linkers and they have become a prominent area in solid-state chemistry (Figure 21). Unlike traditional porous materials such as zeolites and activated carbons, MOFs provide a high degree of functional and structural tunability. Nanoporous materials, with regular organic-inorganic hybrid frameworks, have pores ranging from 0.2×10^{-9} to 100×10^{-9} meters. In contrast, zeolites are inorganic and amorphous, while activated carbon is considered an organic porous material. The types of pores found in porous materials are outlined below (Khan *et al.*, 2021).

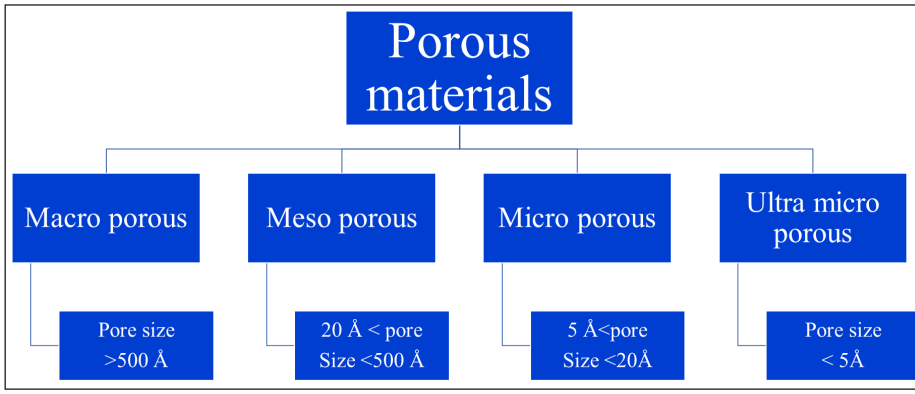

Figure 21: PTypes of pores based on pore size

20. Recent Progress in MOFs for Gas Storage

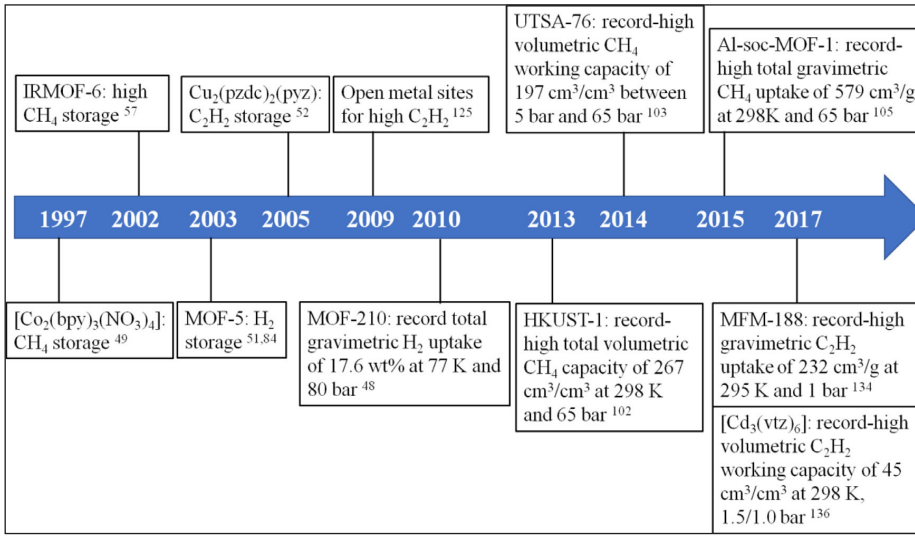

Figure 22: Timeline of important breakthroughs in gas storage using MOFs

20.1. Porous Metal-Organic Frameworks for Gas Storage

i) ZIF-8 is 2-methylimadizole zinc salt of general chemical formula $C_8H_{10}N_4Zn$. The ZIF-8 is $Zn(MeIM)_2$. Here, MeIM is 2-methylimidazolate. The ZIF-8 is composed of zinc atom bonded with 2-methylimidazolate ligands with large cavities (11.4 Å) and small pore (3.4 Å) structures (Bhattarai *et al.*, 2021).

ii) Cu-BTC is copper benzene-1,3,5-tricarboxylate with a chemical formula of $[Cu_3(btc)_2]$ or $C_{16}H_6Cu_3O_{12}$. Here, btc is 1,3,5-benzenetricarboxylate. It is commercially available. It consists of three distinct cages: one small octahedral cage with a pore window of 2.0 Å and pore radius of 5.2 Å. Another larger cage is the cuboctahedral cage with a pore radius of 6.1 Å connected by a pore aperture of 2.6 Å radius (Bhattarai *et al.*, 2021).

20.2. Synthesis of MOFs

Metal-organic frameworks (MOFs) have proven effective for removing volatile organic compounds (VOCs). Their superior surface area, large pore volume and specific gas adsorption capabilities give MOFs an edge over other common adsorbents in VOC removal. Additionally, post-fabrication modifications of MOFs can enhance their selective adsorption properties. MOFs can also be used in the synthesis of nanomaterials for VOC removal. MOFs can be synthesized through various methods, as outlined by Bhattarai *et al.* (2021).

i) Solvothermal or hydrothermal: In this method, crystals gradually develop over several hours to days from a heated solution.

ii) Microwave-assisted solvothermal synthesis: in this method, microwaves can be used to nucleate MOF crystals rapidly from a solution.

iii) Chemical vapor deposition method: This is a solvent-free method for the synthesis of MOFs. In this method, initially, metal oxide precursor layers are deposited, followed by exposing to sublimed ligand molecules, which induces a phase transformation to the MOF crystal lattice.

20.3. MOFs for Pheromone Delivery

The use of MOFs for controlled release of mating disruption agents like pheromones and semiochemicals is a relatively recent development. Zirconium-based MOFs, in particular, show promise for applications involving volatile organic compounds and semiochemicals. According to Doan (2015), three distinct zirconium-based MOFs with various linkers (benzene-1,4-dicarboxylate, 2-aminobenzene-1,4-dicarboxylate and 2-(propylamino)-benzene-1,4-dicarboxylate) were synthesized using a solvothermal method and evaluated for their potential in pheromone delivery. The study used 3-octanone, a model pheromone, which was loaded into these MOFs and analyzed by NMR spectroscopy. The results indicated that the MOFs could hold pheromones in varying amounts. The physical properties of these MOFs, such as surface area, pore volume and crystal density, along with nitrogen adsorption and pheromone diffusion, were extensively studied through simulations. The higher electrostatic interactions in UiO-66-NH_2 result in greater guest-host interaction energies compared to UiO-66, suggesting its potential as a promising material for sustainable agriculture (Figure 23).

Zinc(II) and zirconium(IV) metal-organic frameworks (MOFs) exhibit the ability to absorb and slowly release ant alarm pheromones such as 3-octanone and 4-methyl-3-heptanone. These pheromones have been incorporated into MOFs from the IRMOF and UiO-66 isoreticular series, as well as the coordinatively-unsaturated MOF-74 (Table 6). The MOFs used in these studies were synthesized using established methods, including $[Zn_4O(bdc)_3]$ (IRMOF-1), $[Zn_4O(bdc\text{-}NH_2)_3]$ (IRMOF-3), $[Zn_4O(bdc\text{-}NHPr)_3]$ (IRMOF-NHPr), $[Zn_4O(bdc\text{-}NHBu)_3]$ (IRMOF-NHBu) and $[Zn_4O(bdc\text{-}NHOc)_3]$ (IRMOF-NHOc). For initial studies, 3-octanone was chosen as the pheromone. According to a space-filling model based on the van der Waals radii of the atoms, 3-octanone measures approximately 13.0Å × 5.5Å × 4.2Å, allowing it to easily enter

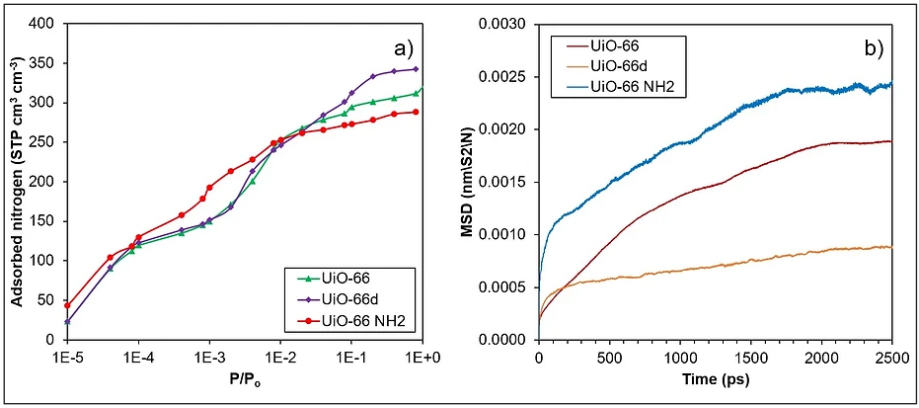

Figure 23: a) Nitrogen adsorption isotherm of MOFs at 77 K (with a logarithmic pressure scale) obtained through Monte Carlo simulations; b) Mean square displacement of 3-octanone within MOFs, calculated using molecular dynamics simulations (Doan, 2015)

the pores of IRMOF-1, which has an approximate pore window of 11.0Å × 11.0Å (Hamzah *et al.*, 2020). Details on the inclusion of 3-octanone (oct) into IRMOFs are provided below.

Table 6: Different types of MOFs and absorptive capacity

MOF	SBET (m^2g^{-1})[20]	Initial analysis[a] % wt uptake	After washing[b] % wt uptake	After washing[c] % wt uptake
IRMOF-1	3800	3.3	0	0
IRMOF-3	2613	6.3	3.1	0
IRMOF-NHPr	1914	23.2	20.5	19.1
IRMOF-NHBu	1862	13.0	13.0	13.0
IRMOF-NHOc	1233	Trace	0	0

[a]One DMF wash; [b]Two DMF washes; [c]Three DMF washes

^{1}H NMR spectroscopy was performed on samples of IRMOF-3, IRMOF-NHPr and MOF-74 that had been impregnated with 3-octanone through solvent exchange (Figure 24). The pheromone-loaded MOFs were exposed to air for nine weeks and samples were collected every few days, digested and analyzed spectroscopically (Hamzah *et al.*, 2020).

Moreno *et al.* (2016) developed 1D nickel-based metal-organic nanoribbons, which feature inorganic metal cluster chains linked by organic spacers composed of monocarboxylic acids. This synthesis produced well-ordered layers capable of expanding and exfoliating when exposed to various solvents. The pheromone 3-(S)-methyl-6-(R, S)-isopropenyl-9-decenyl acetate was incorporated into 2 grams of the material at a loading of 25% by weight. The

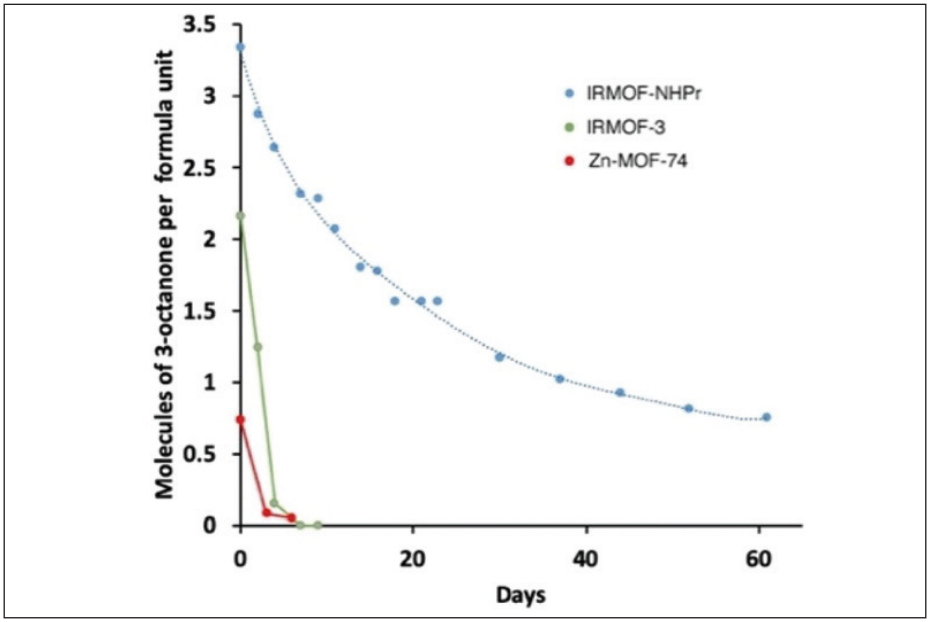

Figure 24: The amount of 3-octanone remaining in the loaded samples of IRMOF-3, IRMOF-NHPr and Zn-MOF-74 after more than 60 days of exposure to air was evaluated using 1H NMR spectroscopic analysis of the digested samples (Hamzah *et al.*, 2020)

release kinetics demonstrated that this material retained only 10% of the loaded pheromone, indicating that it has significant potential for slow and controlled chemical release in pest control applications.

21. Other Type of Nanoscale Pheromone Dispensers

For the controlled release of sex pheromones loaded into monomethoxy poly(ethylene glycol)-poly(ε-caprolactone) [MPEG-PCL] diblock copolymer micelles, specifically (Z,E)-9,11- and (Z,E)-9,12-tetradecadienyl acetate (Z9,E11-14; Z9,E12-14) for *Spodoptera litura* (Lepidoptera: Noctuidae), the optimal encapsulation conditions involved stirring MPEG5000-PCL2000 at 1000 rpm and 30 °C with a 2.5:1 wall-forming to core material mass ratio. The pheromone release was tested in an artificial climate chamber with a controlled temperature of 35±3 °C, a 12-hour light/dark cycle and 75±5% relative humidity over a period of 28 days. To assess the pheromone release from the micelles prepared under these conditions, samples were analyzed daily during the first 14 days and then every 7 days for the remaining 14 days (Chen *et al.*, 2018).

This study evaluates micrometer-sized particles as controlled-release devices for volatilizing insect pheromones used in mating disruption, focusing on two pheromone/ model compound systems: codlemone/1-dodecanol and disparlure/1,2-epoxyoctadecane. Polymer-coated particles are prepared by

dispersing substrates containing the pheromones into aqueous solutions of the specified polymers. Typically, 500 mg of particles is immersed in 20-25 mL of a 5-10 wt% polymer solution and allowed to equilibrate for 1 hour (Figure 24). The "wet" particles are then collected by vacuum filtration on Whatman no. 1 filter paper and dried overnight at room temperature. Particle surface area and pore size are measured using a nitrogen adsorption-desorption isotherm method with a NOVA-1200 gas sorption analyzer (Quantachrome Corp.). Particles coated with 6% HPC (by weight of the total particle mass) show a reduction in release rate of 16-28% across the temperature range studied, while an 8% HPC coating results in nearly 40% reduction in release rate (Stipanovic *et al.*, 2004).

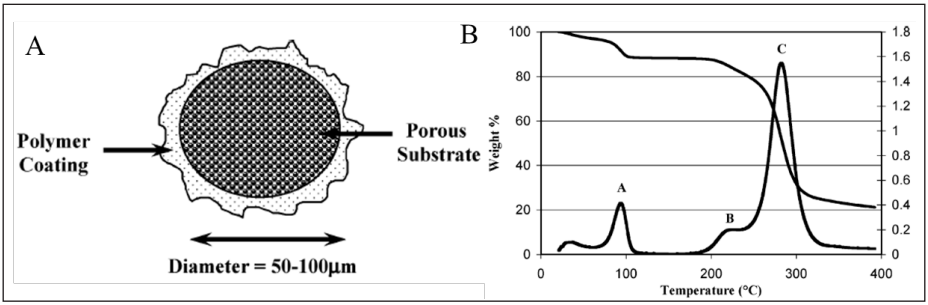

Figure 24: (A) Porous substrate coated with polymer. (B) Dynamic TGA analysis of dodecanol adsorbed onto MCC coated with a water-soluble polymer: (A) evaporation of dodecanol, (B) degradation of the coating and (C) pyrolysis of cellulose. The upper curve represents the actual weight loss thermogram, while the lower curve shows the first derivative of the thermogram with respect to temperature

Molecular gels demonstrate their potential as efficient controlled release systems for pheromones, which could serve as biopesticides. These innovative devices are easily biodegradable, have a high capacity for pheromone loading and provide a sustained release of the pesticide at elevated concentrations over an extended period (Jadhav *et al.*, 2010). In a similar vein, Hellmann *et al.* (2009) developed pheromone-releasing nanofibers for plant protection using electrospinning techniques with polyamide. This method produced fibers that expanded their release over several weeks to months. By electrospinning a solution containing polyamide 6 and various concentrations of pheromone, they created smooth nanofibers with diameters ranging from 150 to 600 nm and ribbons from 600 to 1500 nm. The electrospun fibers showed a similar morphology to polyamide fibers spun from formic acid without pheromone content (Figure: 26). The pheromone begins to vaporize at around 110 °C and is completely vaporized by approximately 250 °C, while the polyamide remains stable within this temperature range, allowing TGA analysis to determine the total amount of pheromone present. The nanofibers can incorporate up to 33 wt% pheromone, which may undergo nanoscale phase separation during the electrospinning process.

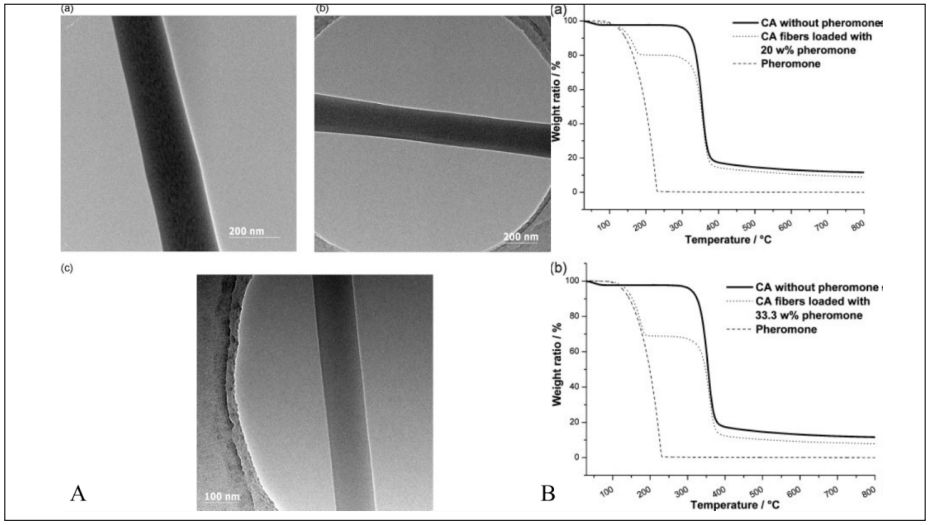

Figure 25: (Electrospun nanofibers: (A) Transmission electron microscopy images of cellulose acetate nanofibers with dispersed pheromone at the following loadings: (a) 20 wt%, (b) 33.3 wt% (from the solution) and (c) 0 wt%. (B) Thermogravimetric analysis (TGA) curves for cellulose acetate nanofibers, pure pheromone and pheromone-loaded cellulose acetate nanofibers with contents of: (a) 20 wt% and (b) 33.3 wt% in the spinning solution (Hellmann et al., 2009).loss thermogram, while the lower curve shows the first derivative of the thermogram with respect to temperature

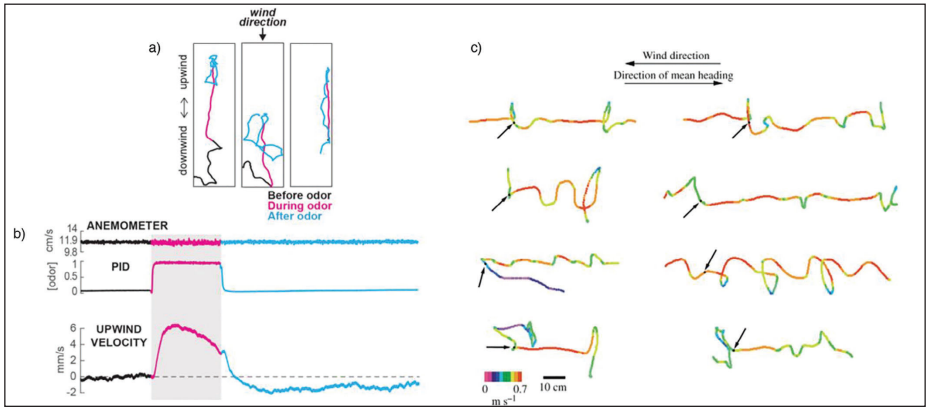

Figure 26: The movement patterns of fruit flies in response to an attractive odor, both with and without its presence, are examined. (a) Walking paths and (b) movement speeds of three different fruit flies are recorded during ON and OFF phases of exposure to the odor, with data collected before (black), during (magenta) and after (blue) a 10-second odor pulse. (c) The flight patterns and speeds of fruit flies are analyzed during the release of the attractive odor, with the onset indicated by a black arrow.

22. Insect Behavior and Pheromones

Traces of volatile semiochemicals elicit species-specific reactions, such as insects moving towards or away from the release source. Insects detect these volatile chemicals through olfactory receptor neurons, which have varying levels of specificity (De Bruyne and Baker, 2008). Among the different designs for such assays, flight tunnels are the most frequently used (Figure 27). Research has shown that moths quickly respond to changes in pheromone concentrations emitted from a point source. Their flight paths can become zigzagging or linear, depending on the concentration patterns of the pheromone plume, whether it is continuous, pulsed or turbulent (Álvarez-Salvado *et al.*, 2018; Geier *et al.*, 1999).

23. Conclusion

Insect pheromones are defined by their carbon count, functional groups, double bond arrangements and the ratio of major to minor compounds. Advances in analytical and electrophysiological methods have made it easier to isolate, identify and synthesize these semiochemicals for field applications. Methyl eugenol, cuelure and trimedlure are widely used parapheromones for purposes such as monitoring, mass trapping and male annihilation.

24. References

Álvarez-Salvado, E., Licata, A.M., Connor, E.G., McHugh, M.K., King, B.M.N., Stavropoulos, N., Victor, J.D., Crimaldi, J.P., Nagel, K.I., 2018. Elementary sensory-motor transformations underlying olfactory navigation in walking fruit-flies. *eLife* 7, e37815. DOI: https://doi.org/10.7554/eLife.37815.

Anderson, A.R., Wanner, K.W., Trowell, S.C., Warr, C.G., Jaquin-Joly, E., Zagatti, P., Robertson, H., Newcomb, R.D., 2009. Molecular basis of female-specific odorant responses in *Bombyx mori*. *Insect Biochemistry and Molecular Biology* 39(3), 189-197. DOI: https://doi.org/10.1016/j.ibmb.2008.11.002.

Augusto, F., Valente, A.L.P., 2002. Applications of solid-phase microextration to chemical analysis of live biological live. *TrAC Trends Anal. Chem.* 21(6-7), 428-438. DOI: https://doi.org/10.1016/S0165-9936(02)00602-7.

Baker, T.C., Roelofs, W.L., 1981. Initiation and termination of oriental fruit moth male response to pheromone concentrations in the field. *Environ. Entomol.* 10(2), 211-218. DOI: https://doi.org/10.1093/ee/10.2.211.

Bhattarai, D.P., Pant, B., Acharya, J., Park, M., Ojha, G.P., 2021. Recent progress in metal-organic framework-derived nanostructures in the removal of volatile organic compounds. *Mol.* 26, 4948.

Chen, Y., Chen, X., Chen, Y., Wei, H., Lin, S., Tian, H., *et al.*, 2018. Preparation, characterization and controlled release of sex pheromone-loaded MPEG-PCL diblock copolymer micelles for *Spodoptera litura* (Lepidoptera: Noctuidae). *PLoS ONE* 13(9), e0203062.

Coffey, J.L., Simmons, A.M., Shepard, B.M., Levi, A., 2016. Vertical Y-tube assay for evaluation of arthropod response to plant materials. *J. Agril.*

Urban Entomol. 32, 7-12.

Das, P.P., 2021. Fabrication of a vertical Y-tube olfactometer for the assessment of spatial repellency of essential oils against *Helopeltis theivora* waterhouse. *Int. J. Tropical Insect Sci.* 42, 835-844. DOI: https://doi.org/10.1007/s42690-021-00607-3.

De Bruyne, M., Baker, T.C., 2008. Odor detection in insects: Volatile codes. *J. Chem. Ecol.* 34, 882-897.

Doan, H., 2015. Synthesis of zirconium-based MOFs for pheromones delivery: A study on NMR and molecular simulation. Available at: https://www.huandoan.co.uk/post/2015/09/24/using-metalorganic-frameworks-for-the-targeted-delivery-of-pheromones-and-pesticides-1.

Geier, M., Boeckh. J., 1999. A new Y-tube olfactometerfor mosquitoes to measure the attractiveness of hostodors. *Entomol. Exp. Appl.* 92, 9-19.

Geier, M., Bosch, O.J., Boeckh, J., 1999. Influence of odour plume structure on upwind flight of mosquitoes towards hosts. *J. Exp. Biol.* 202(12), 1639-1648.

Ghosh, S.K., 2019. Metal-Organic Frameworks (MOFs) for environmental applications. Elsevier, Amsterdam. pp. 8-13.

Greiner, A., Wendorff, J.H., 2007. Electrospinning: A fascinating method for the preparation of ultrathin fibers. *Angewandte Chemie International Edition* 46, 5670-5703. DOI: https://doi.org/10.1002/anie.200604646.

Hellmann, C., Greiner, A., Vilcinskas, A., 2023. Design of polymer carriers for optimized pheromone release in sustainable insect control strategies. *Adv. Sci.* 11, 2304098.

Hellmann, C., Greiner, A., Wendorff, J.H., 2011. Design of pheromone releasing nanofibers for plant protection. *Polym. Adv. Technol.* 22, 407-413. DOI: https://doi.org/10.1002/pat.1532.

Hellmanna, C., Greinera, A., Wendorff, J.H., 2009. Design of pheromone releasing nanofibers for plant protection. *Poly. Adv. Technol.* 22, 407-413.

Kainoh, Y., 2011. Wind tunnel: A tool to test the flight response to semiochemicals. In: *Wind Tunnels and Experimental Fluid Dynamics Research*. (Eds.) Lerner, J.C. and Boldes, U. Intechopen. DOI: https://doi.org/10.5772/730.

Kainoh, Y., Hiyori, T., Ninomiya, Y., 1984. Conditions for wind tunnel tests in studying pheromonal communication in the smaller tea tortrix moth, *Adoxophyes* sp. (Lepidoptera: Tortricidae). *Appl. Entomol. Zool.* 19, 526-528.

Khan, A., Jawaid, M., Asiri, A.M.A., Ni, W., Rahman, M.M., 2021. Metal-organic framework nanocomposites from design to application. CRC Press, Abingdon, Oxon. pp. 5-15.

Li, Y.Y., Liu, D., Wen, P., Chen, L., 2021. Detection of volatile organic compounds by *Antennal lamellae* of a scarab beetle. *Front. Ecol. Evol.* 9, 759778. DOI: https://doi.org/10.3389/fevo.2021.759778.

Lu, Y., Liu, Q., 2022. Insect olfactory system inspired biosensors for odorant detection. *Sens. Diagn.* 1, 1126.

Lukasz, L.S., Miller, J.R., Larry J.G., 2003. Presence of long-lasting peripheral adaptation in oblique-banded leaf roller, *Choristoneura rosaceana* and absence of such adaptation in red banded leaf roller, *Argyrotaenia velutinana*. *J. Che. Ecol.* 29(2), 405-423.

McCaffery, A.R., Wilson, I.D., 1990. Chromatography and isolation of insect hormones and pheromones. Plenum press, New York and London. pp. 287-300.

Millar, J.G., Haynes, K.F., 2000. *Methods in Chemical Ecology: Chemical Methods*, 2nd Edition. Chapman & Hall, London. pp. 50-65.

Moreno, J.M., Navarro, I., Díaz, U., Primo, J., Corma, A., 2016. Single-layered hybrid materials based on 1D associated metalorganic nanoribbons for controlled release of pheromones. *Angew. Chem. Int. Ed.* 55, 11026-11030.

Obermayr, U., Ruther, J., Bernier, U., Rose, A., Geier, M., 2012. Laboratory evaluation techniques to investigate the spatial potential of repellents for push and pull mosquito control systems. *Entomol. Soc. America*, 0022-2585/12/1387Ð1397$04.00/0.

Patt, J., Setamou, M., 2010. Responses of the Asian citrus psyllid to volatiles emitted by the flushing shoots of its rutaceous host plants. *Environ. Entomol.* 39, 618-624. DOI: https://doi.org/10.1603/EN09216.

Pawson, S.M., Kerr, J.L., O'Connor, B.C., Lucas, P., Martinez, D., Allison, J.D., Strand, T.M., 2020. Light-weight portable electroantennography device as a future field-based tool for applied chemical ecology. *J. Chem. Ecol.* 46, 557-566.

Stipanovic, A.J., Hennessy, P.J., Webster, F.X., Takahashi, Y., 2004. Microparticle dispensers for the controlled release of insect pheromones. *J. Agric. Food Chem.* 52, 2301-2308.

WHO, 2013. Guidelines for efficacy testing of spacial repellents. WHO, Switzerland.

Yew, J.Y., Chung, H., 2015. Insect pheromones: An overview of function, form and discovery. *Prog. Lipid Res.* 59, 88-105.

Zhang, P.J., Liu, S.S., Wang, H., Zalucki, M.P., 2007. The influence of early adult experience and larval food restriction on responses toward nonhost plants in moths. *J. Chem. Ecol.* 33, 1528-1541.